energies

MDPI

Article

Numerical Model of Heat Pipes as an Optimization Method of Heat Exchangers

Łukasz Adrian *, Szymon Szufa *, Piotr Piersa and Filip Mikołajczyk

Faculty of Process and Environmental Engineering, Lodz University of Technology, Wolczanska 213, 90-924 Lodz, Poland; Piotr.piersa@p.lodz.pl (P.P.); filip.mikolajczyk@p.lodz.pl (F.M.)

* Correspondence: lukasz.adrian@p.lodz.pl (Ł.A.); szymon.szufa@p.lodz.pl (S.S.); Tel.: +48-501-156-231 (Ł.A.); +48-606-134-239 (S.S.)

Abstract: This paper presents research results on heat pipe numerical models as optimization of heat pipe heat exchangers for intensification of heat exchange processes and the creation of heat exchangers with high efficiency while reducing their dimensions. This work and results will allow for the extension of their application in passive and low-energy construction. New findings will provide a broader understanding of how heat pipes work and discover their potential to intensify heat transfer processes, heat recovery and the development of low-energy building engineering. The need to conduct research and analyses on the subject of this study is conditioned by the need to save primary energy in both construction engineering and industry. The need to save primary energy and reduce emissions of carbon dioxide and other pollutants has been imposed on the EU Member States through multiple directives and regulations. The presented numerical model of the heat pipe and the results of computer simulations are identical to the experimental results for all tested heat pipe geometries, the presented working factors and their best degrees of filling.

Keywords: heat pipe; heat transfer; heat exchanger; phase change; evaporation; condensation; low emission; numerical model

Citation: Adrian, Ł.; Szufa, S.; Piersa, P.; Mikołajczyk, F. Numerical Model of Heat Pipes as an Optimization Method of Heat Exchangers. *Energies* **2021**, *14*, 7647. https://doi.org/10.3390/en14227647

Academic Editor: Manabendra Saha

Received: 3 October 2021
Accepted: 6 November 2021
Published: 16 November 2021

1. Introduction

Climate neutrality and the decoupling of economic growth from the consumption of natural resources are the two goals set out in the European Green Deal, i.e., the EU's strategy for achieving zero greenhouse gas emissions by 2050 [1]. The EU action plan concerns the transformation of areas such as food, energy, transport, industry, construction and ecosystems where most heat exchangers are used, and their optimization will positively affect the energy efficiency of these sectors. The obtained results enable the intensification of heat exchange processes and the creation of heat exchangers with high efficiency while reducing their dimensions. The research results of this study will allow for the extension of their application, among others, in passive and low-energy construction. Research results provide a broader understanding of how heat pipes work to discover their potential to intensify heat transfer processes, heat recovery and the development of low-energy building engineering [2]. The research results allow for the extension of applications in passive and low-energy construction. The need to conduct research and analyses on the subject of this study is also conditioned by the need to save primary energy in both construction engineering and industry. The need to save primary energy and reduce emissions of carbon dioxide and other pollutants has been imposed on the EU Member States through multiple directives and regulations. Among other things, the European Union introduced the so-called "Climate Package", which is a set of binding rules to ensure that the EU meets its climate and energy goals [3]. The advantages of using heat pipes are to significantly increase the efficiency of devices collecting heat from lower renewable energy sources, such as soil or heat storage, which perfectly fits in activities limiting the consumption of primary energy and increasing energy efficiency. The conclusions of this

study also confirm the possibility of heat pipe operation in a wide temperature range and the ability to work at even the smallest temperature differences, which will certainly contribute to more efficient renewable sources and allow their use in places, so far, limited by investment profitability. As a result, heat pipes can be widely used in heat pumps, air conditioning, refrigeration, heating, ventilation, construction engineering and solar energy [4].

Few devices play as important a role as heat exchangers in the pursuit of optimization and energy savings. Installations of high-efficiency heat exchanger systems open up completely new opportunities to reduce energy costs and CO_2 emissions without compromising the performance and quality of the final product [5].

This study clearly indicates that the installation of more efficient heat exchangers is often the best way to remove limitations caused by insufficient thermal or cooling capacity. More efficient heat flow means more energy goes into the manufacturing process, increasing the available production capacity while reducing costs.

Computer simulations, which are the subject of this study, were carried out on a 1769 mm long heat pipe exchanger made of copper, with an 18 mm outside diameter and a 1 mm wall thickness (Tube 1). The exchanger was made of copper due to its high thermal conductivity and availability. The length was selected so that the heat receiving and dissipating parts were in the middle of the 0.5–1 m range, which corresponds to a typical series of heights of ventilation and air-conditioning ducts and units. As part of the subject of this work, experimental tests of a heat pipe made of brass, 550 mm long, with a 22 mm outer diameter, and a 1 mm wall thickness (Tube 2), were also carried out at the Thermal Technology Department of the Fluid Flow Machinery Institute of the Lodz University of Technology, the results and conclusions of which are taken into account in the comparative analysis in this work [6].

2. Materials and Methods

2.1. Used Materials and Their Properties

ANSYS Design Modeler was used in the ANSYS FLUENT™ (ANSYS, Inc., 2600 Ansys Drive, Canonsburg, PA 15317, USA) software package to create a representative model of a two-dimensional tube-in-tube heat exchanger, which was used to simulate the process parameters during its operation. Due to the cylindrical shape of the apparatus and the axes of symmetry occurring in it, it was possible to use a two-dimensional model instead of a three-dimensional one, which reduced the required computing power and time, as well as a denser computational mesh. When creating the mesh, the ANSYS Mesh software was used, and the mesh shape was assumed to be rectangular with a local density close to the interface. This made it possible to model the flow and heat transfer in the heat pipe as accurately as possible. The increased density was assumed to be 2 mm from the wall; further compaction of the mesh did not bring significant changes in the calculation results. Figure 1 shows the modeled geometry and mesh. In the area of the fluid, 60,690 nodes and 29,118 elements were created, while in the area of the solid body (walls), 9816 node oras of 3678 elements were applied. The simulations were carried out for both a 1769 mm long copper pipe and a 550 mm long brass one. The simulation was carried out for the most favorable degree of liquid filling obtained during a series of experimental tests. The simulation was assumed to be closed, i.e., the influence of external factors was not taken into account. In real conditions, such an arrangement would correspond to the thermal insulation of the apparatus, e.g., in the form of a cover.

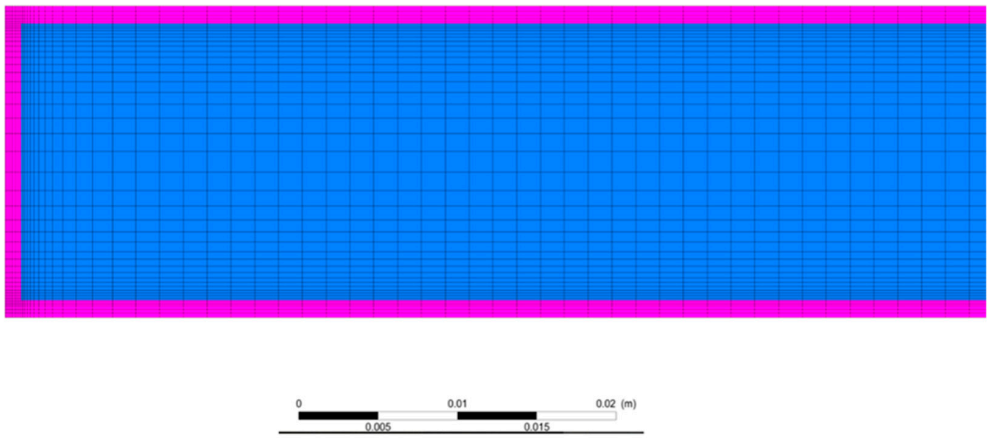

Figure 1. Geometry and mesh of the modeled heat pipe.

The ANSYS CFD and ANSYS Fluent software were used to simulate the operation of the heat exchanger. Based on the performed laboratory experiments, the start-up parameters for the simulation were selected. The water flow was constant at 15 L/h. The starting temperature of the hot liquid was 10 °C, and the hot liquid was 50 °C. Fluid end temperatures were not assumed; they were the result of the simulations. Water was used as the heating and cooling liquid. As for the working factors of the heat pipes, three basic ones available on the market were adopted. After a thorough analysis of thermodynamic properties and market applications, refrigerants in the form of R134A, R404A and R407A were selected.

The refrigerant R134A (1,1,1,2-tetrafluoroethane) was chosen because of its wide use in refrigeration appliances and small- and medium-scale air conditioners. It was introduced as a replacement for R12 and R500 due to their destructive effect on the ozone layer. Over the years, it has been widely used in household appliances and the automotive industry, but due to its potentially harmful impact on the environment (ozone depletion and the possibility of creating acid rain), it is beginning to be replaced by other substances such as R134yd, R450 and R513A. Its optimal use is at low and high temperatures. Due to the irritating smell and higher density than air, it is necessary to apply appropriate safety measures.

R404A refrigerant is a mixture of R143A (52%), R125 (44%) and R134A (4%). It is widely used in low-, wide- and high-temperature refrigeration. It was introduced as a replacement for the R502, R22 and R507, and has found wide application in many branches of the economy. There is industrial refrigeration, where it is used in cold stores and freezers, commercial refrigeration, for example, in the form of cold stores, refrigerated shelves with food, restaurant or hotel air conditioners, as well as in the automotive industry, where it is used in transport vehicles.

R407C is one of the proposed alternatives to R404A, which is quite similar in terms of refrigeration properties but has a much lower GWP value and is non-flammable and less toxic. This refrigerant is a mixture of the refrigerants R32 (23%), R125 (25%) and R134A (52%), with a composition similar to R407A, but in terms of pressure, it is closer to R22. It is widely used in cold stores, air conditioners, heat pumps and transport.

CFD simulation corresponds to an experimental installation that was made for two types of materials. The first is copper, due to its high heat transfer coefficients, availability and wide applications in the refrigeration industry. The chosen tube geometry also corresponds to those found in common devices. The height of the copper tube was 1769 mm, the internal diameter was 16 mm, and the wall thickness was 1 mm. The second tube was made of brass, 550 mm high, with an internal diameter 16 mm and a wall thickness of 1 mm. For both tubes, the geometry was accurately mapped in the software. The absence of friction and fluid slip on the surface of the walls was assumed, smooth walls were assumed geometrically without local changes in diameter. The properties and physico-

chemical parameters of the materials were adopted from the configurator built into the ANSYS package, where ready profiles were selected, taking into account changes in fluid parameters with temperature and pressure. The same was done in the case of fluids used in the simulation.

Due to the desire to recreate the real, experimental working conditions of the device, different amounts of working factors were adopted for each of the systems, as in Table 1. The remaining part of the tube filling was a vacuum. These values were selected for each of the systems on the basis of laboratory tests, where the highest values of absorbed and returned heat were obtained for the assumed values [6]. This allowed for the most optimal operation of the device and the achievement of the highest efficiency and effectiveness rates of the devices.

Table 1. Values adopted in the simulation of the content of working factors.

Coolant	Amount of Coolant in the Pipe [%]	
	Copper Pipe	Brass Pipe
R134A	10	10
R404A	10	10
R407C	5	30

2.2. Research Methodology

When designing the simulation, some simplifications and assumptions were made to reduce the load on the computer equipment while maintaining the most faithful representation of the processes taking place in the exchanger. Due to the shape of the exchanger, it was possible to simulate two-dimensional geometry instead of three-dimensional. Moreover, it was decided to ignore the effects related to the flow of water washing the heat pipe. This was solved by setting the temperature on the surface of the outer wall of the heat tube (Figure 2). Such a procedure allowed for the elimination of random temperature changes on the walls (caused, among others, by local turbulence in the flow), which positively translated into the repeatability of the process results. An additional advantage is the lack of need to bring the liquid flow to a steady state in the exchangers, which significantly shortens the simulation. Moreover, the results obtained for water are not important from the point of view of simulating the flow inside the heat pipe.

After conducting a series of simulations to verify the usability of mathematical computational models embedded in the software, it was decided that the K-Omega SST model best describes the selected issue. This is mainly due to the very good description of the boundary issues from other tested models. Due to the fact that the mechanism of operation of the heat pipe described in the article is based mainly on the processes taking place in this area, this model allows for the most faithful representation of the actual behavior of the pipe. Moreover, during the test analyses, it was shown that the achieved real velocities of fluids inside the tube did not exceed 0.3 m/s; therefore, it was possible to further simplify the simulation. The values of criterion numbers, such as the Reynolds and Grasshof numbers, for the fluid test parameters determined during the simulations indicated that for the adopted geometry and physicochemical properties of the fluid, the flow was not fully turbulent even under the most optimal conditions. Thanks to this, in the further part of the simulation, the developed turbulence model was not adopted. On the basis of observations during tests of the actual installation, it was found that no chemical reactions occurred inside the heat pipe during the operation of the exchanger. As a result, the model of a two-phase two-component mixture was selected, taking into account the phase change. Due to the lack of observation of the phenomenon during practical tests and test simulations, cavitation was not included in the analysis in order to avoid potential errors.

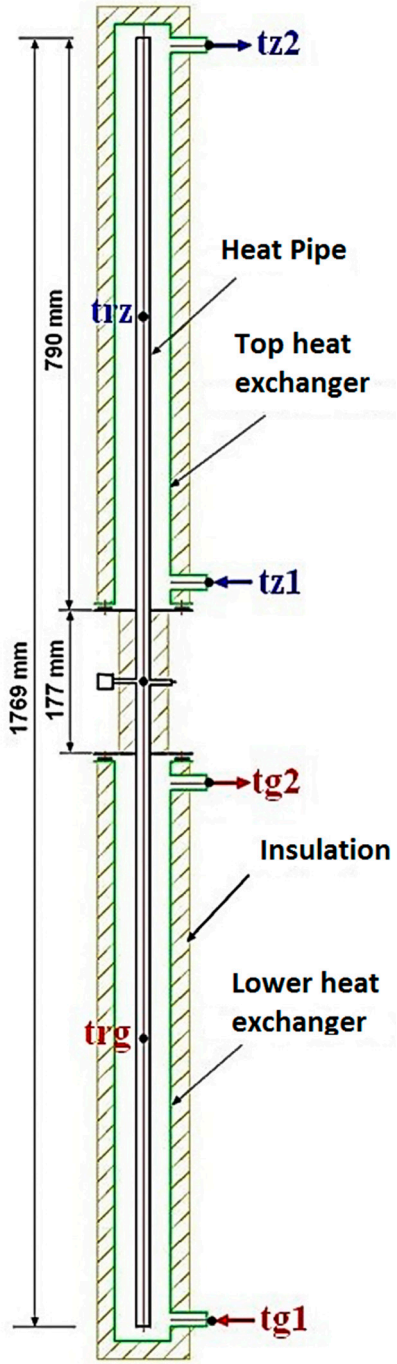

Figure 2. Scheme of the installation of the heat pipe at the measuring stand with temperature measurement points [6].

The hot medium flow takes place on the walls of the evaporator, in the lower part of the device, where the hot liquid is introduced at the bottom of the device and flows upwards. The flow of cold liquid in the upper exchanger is analogous. The analyzed heat pipe is located in the middle of the structure. It was assumed that the tube walls were completely smooth, and any effects related to apparatus roughness were neglected. Due to the vertical structure of the apparatus, the simulation takes into account the influence of gravity on the behavior of fluids. Due to the insulation used in the experimental equipment in the pipe section between the heat exchangers, it was assumed that the outer walls of this section are adiabatic walls.

The boundary conditions of the simulation were selected on the basis of the conducted laboratory experiments. This made it possible to compare the simulation results with

the actual results, and thus, to verify the model assumed in the simulation. The initial temperature of the external walls in the upper exchanger was taken as 10 °C, and the wall temperature in the lower exchanger was taken as 50 °C.

During the simulation, the model of a two-phase system was used due to the occurrence of the phase transformation of the working media. For this purpose, tools and algorithms embedded in the software were used. The description of fluid movement in the adopted model was based, inter alia, on a standard set of mass and momentum conservation equations.

$$\frac{\partial \rho}{\partial t} + \nabla \cdot \left(\rho \vec{v} \right) = S_m \tag{1}$$

$$\frac{\partial}{\partial t}\left(\rho \vec{v} \right) + \nabla \cdot \left(\rho \vec{v} \vec{v} \right) = -\nabla p + \nabla \cdot \left(\bar{\bar{\tau}} \right) + \rho \vec{g} + \vec{F} \tag{2}$$

where S_m is the volume source, τ is the stress tensor, g is the acceleration of gravity, F is the external force acting on the fluid. The aforementioned occurrence of phase transformations forced the necessity to apply an appropriate multi-phase model. Its absence could cause local anomalies that would make it impossible to obtain reliable and repeatable results. The multi-phase model used in the simulation is based on the Volume of Fluid algorithm:

$$\frac{1}{\rho_q}\left[\frac{\partial}{\partial t}(\alpha_q \rho_q) + \nabla \cdot (\alpha_q \rho_q \vec{v_q}) = S_{\alpha_q} + \sum_{p=1}^{n} \left(\dot{m}_{pq} - \dot{m}_{qp} \right) \right] \tag{3}$$

where α_q is the volume fraction of the q-phase in the cell, m_{pq} and m_{qp} are the mass flows between the phases (due to phase change). The phase change was implemented using the Evaporation/Condensation model. It works on the basis of two dependencies. If the liquid temperature T_l is higher than the saturation temperature T_{sat}, the volumetric mass source is (evaporation):

$$\dot{m}_{lv} = coef\ f \cdot \alpha_l \rho_l \frac{(T_l - T_{sat})}{T_{sat}} \tag{4}$$

If the gas temperature T_g drops below T_{sat}, the liquid mass source (condensation) is:

$$\dot{m}_{vl} = coef\ f \cdot \alpha_v \rho_v \frac{(T_{sat} - T_v)}{T_{sat}} \tag{5}$$

The indices v and l in the above formulas represent vapor and liquid, respectively. *Coef f* is an empirical coefficient that has been assumed to be at a default value of 0.3. The model also takes into account the heat of the phase change, which is calculated as the product of the heat of change times the volumetric source of mass. The saturation temperature depended on the local cell pressure $T_{sat} = f\ (p)$. The software uses separate mathematical models for liquid and solid phases. In the case of fluids, the Navier-Stokes equations are the basis for calculations based on the mass, moment and energy exchange:

$$\frac{\partial \rho}{\partial t} + \frac{\partial (\rho u_i)}{\partial x_i} = 0 \tag{6}$$

$$\frac{\partial (\rho u_i)}{\partial t} + \frac{\partial}{\partial x_j}(\rho u_i u_j) + \frac{\partial P}{\partial x_i} = \frac{\partial}{\partial x_j}(\tau_{ij} + \tau_{ij}^R) + S_i \tag{7}$$

$$\frac{\partial \rho H}{\partial t} + \frac{\partial \rho u_i H}{\partial x_i} = \frac{\partial}{\partial x_i}(u_j(\tau_{ij} + \tau_{ij}^R) + q_i) + \frac{\partial p}{\partial t} - \tau_{ij}^R \frac{\partial u_i}{\partial x_j} + \rho \varepsilon + S_i u_i + Q_H \tag{8}$$

$$H = h + \frac{u^2}{2} \tag{9}$$

In the case of compressible flow, the following equation is additionally taken into account:

$$\frac{\partial \rho E}{\partial t} + \frac{\partial \rho u_i \left(E + \frac{p}{\rho}\right)}{\partial x_i} = \frac{\partial}{\partial x_i}(u_j(\tau_{ij} + \tau_{ij}^R) + q_i) - \tau_{ij}^R \frac{\partial u_i}{\partial x_j} + \rho\varepsilon + S_i u_i + Q_H \tag{10}$$

$$E = e + \frac{u^2}{2} \tag{11}$$

In the case of the laminar flow analysis, the solver is based on the Navier-Stokes equations simplified by Favre, and in the case of turbulent calculations, the *k*-epsilon model is used:

$$\frac{\partial \rho k}{\partial t} + \frac{\partial \rho k u_i}{\partial x_i} = \frac{\partial}{\partial x_i}\left(\left(\mu + \frac{\mu_t}{\sigma_k}\right)\frac{\partial k}{\partial x_i}\right) + \tau_{ij}^R \frac{\partial u_i}{\partial x_j} - \rho\varepsilon + \mu_t P_B \tag{12}$$

$$\frac{\partial \rho \varepsilon}{\partial t} + \frac{\partial \rho \varepsilon u_i}{\partial x_i} = \frac{\partial}{\partial x_i}\left(\left(\mu + \frac{\mu_t}{\sigma_\epsilon}\right)\frac{\partial \varepsilon}{\partial x_i}\right) + C_{\varepsilon 1}\frac{\varepsilon}{k}\left(f_1 \tau_{ij}^R \frac{\partial u_i}{\partial x_j} + C_B \mu_t P_B\right) - f_2 C_{\varepsilon 2}\frac{\rho\varepsilon^2}{k} \tag{13}$$

$$\tau_{ij} = \mu s_{ij} \tag{14}$$

$$\tau_{ij}^R = \mu_t s_{ij} - \frac{2}{3}\rho k \delta_{ij} \tag{15}$$

$$s_{ij} = \frac{\partial u_i}{\partial x_j} + \frac{\partial u_j}{\partial x_i} - \frac{2}{3}\delta_{ij}\frac{\partial u_k}{\partial x_k} \tag{16}$$

$$P_B = -\frac{g_i l}{\sigma_B \rho}\frac{\partial \rho}{\partial x_i} \tag{17}$$

$$\mu_t = f_\mu . \frac{C_\mu \rho k^2}{\varepsilon} \tag{18}$$

$$f_\mu = \left(1 - e^{-0.025 R_y}\right)^2 \cdot \left(1 + \frac{20.5}{R_t}\right) \tag{19}$$

$$R_y = \frac{\rho\sqrt{k}y}{\mu} \tag{20}$$

$$R_t = \frac{\rho k^2}{\mu\varepsilon} \tag{21}$$

$$f_1 = 1 + \left(\frac{0.05}{f_\mu}\right)^3 \tag{22}$$

$$f_2 = 1 - e^{R_t^2} \tag{23}$$

Thermal calculations for fluids are based on the equation:

$$q_i = \left(\frac{\mu}{Pr} + \frac{\mu_t}{\sigma_c}\right)\frac{\partial h}{\partial x_i},\ i = 1, 2, 3 \ldots \tag{24}$$

In the case of solids, the heat transfer is based on the equation:

$$\frac{\partial \rho e}{\partial t} = \frac{\partial}{\partial x_i}\left(\lambda_i \frac{\partial T}{\partial x_i}\right) + Q_H \tag{25}$$

In the case of using a grid that is based on Cartesian coordinates, a problem with the resolution of the interphase layer can be observed. In order to be able to use a solver based on the Navier-Stokes equations, it is necessary to apply the methodology of calculations in the interfacial layer proposed by Prandtl. This is expressed by the Two-Scale Wall Function (2SWF) methodology, which is based on the following assumptions:

- Methodology of "thin" interfacial layers, when the number of cells in the interfacial layer is not sufficient to determine the temperature and flow profiles;
- Methodology of "thick" interfacial layers, when the number of cells in the interphase layer is sufficient for the correct determination of the above-mentioned values;
- Indirect methodology, combining the features of both models.

The model of "thin" interfacial layers is based on the equation:

$$\frac{\partial k}{\partial y} = 0 \tag{26}$$

$$\varepsilon = \frac{C_{\mu}^{0.75} k^{1.5}}{\kappa y} \tag{27}$$

The model of "thick" interfacial layers is based on the Van Driest equation:

$$u^{+} = \int_{0}^{y^{+}} \frac{2 \cdot d\eta}{1 + \sqrt{1 + 4 \cdot \kappa^2 \cdot \eta^2 \cdot \left[1 - exp\left(-\frac{\eta}{A_v}\right)\right]^2}} \tag{28}$$

3. Results

Below are the results of computer simulations based on the numerical model of the heat pipe presented above. The results show graphical temperature distributions inside the heat pipe during its operation for the assumed boundary conditions. Then, the speeds of the working medium inside the heat pipe and the volume fraction of the working medium vapor are presented in order to be able to notice and eliminate the limitations of the heat pipes. Then, for the tested heat pipes, graphs are presented showing the temperature distribution along the central line of the heat pipe and along its wall, as well as a graph showing the temperature distribution along the cross-section. The simulations were carried out for the geometry of the heat pipes indicated in this work and for the experimentally tested working media.

3.1. Pipe I

3.1.1. Air

The results on a closed heat pipe with air in the center forced in at a temperature of 20 °C at atmospheric pressure proved the negligible heat transfer through the heat pipe. As can be seen in Figures 3–6, there are no visible signs that would indicate the occurrence of phase transformations important for the process. These transformations are the driving force of the heat transfer process in the heat pipe, so their absence justifies its malfunction. It is justified by the low thermal conductivity of the air, which, in the tested case, does not act as a conductor, but as an insulator. The obtained results indicate the nec essity to use a different heat transfer medium in the tube.

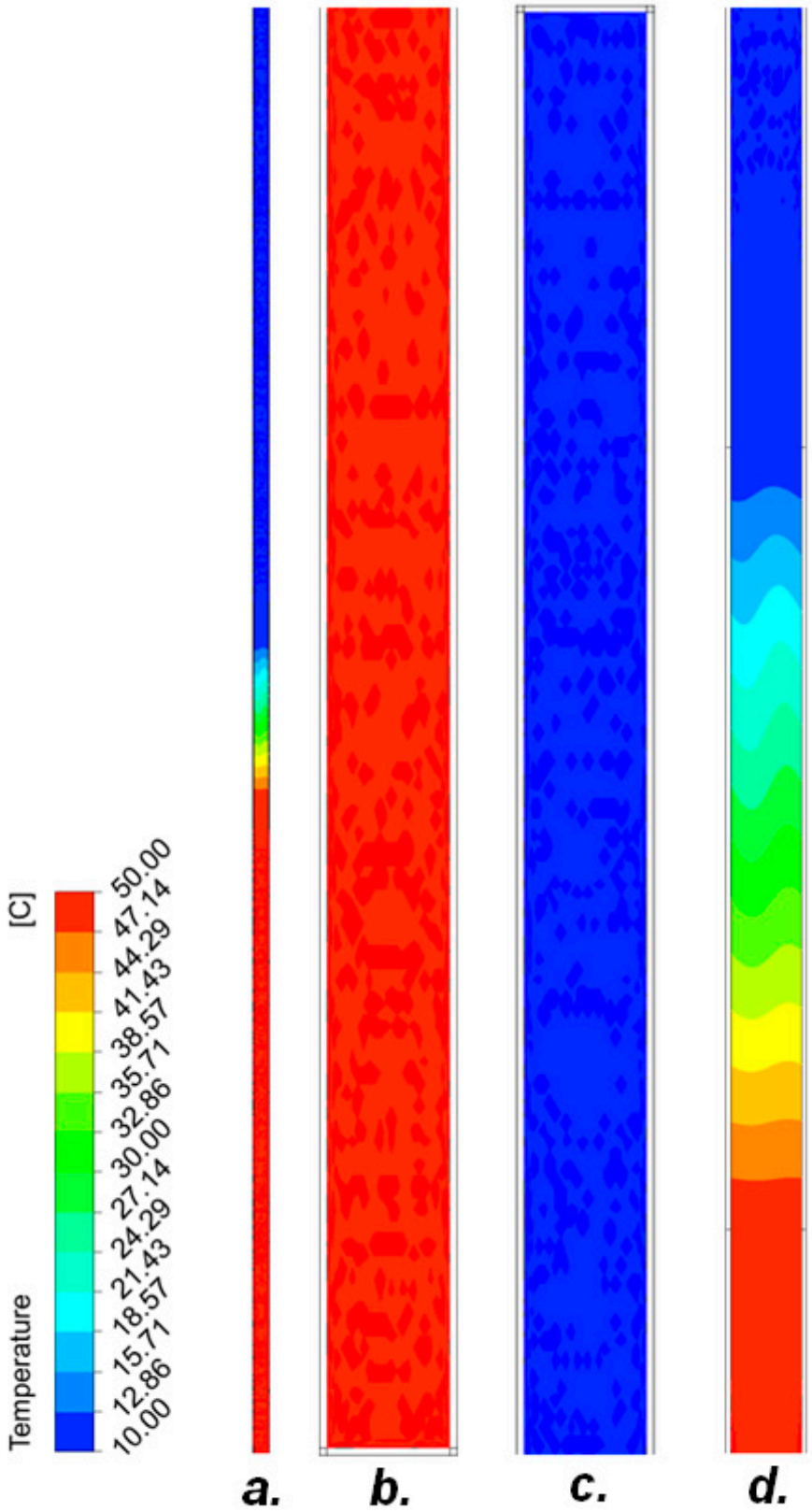

Figure 3. Temperature distribution in the heat pipe. (**a**) Total heat pipe; (**b**) evaporator section; (**c**) condenser section, (**d**) isothermal section.

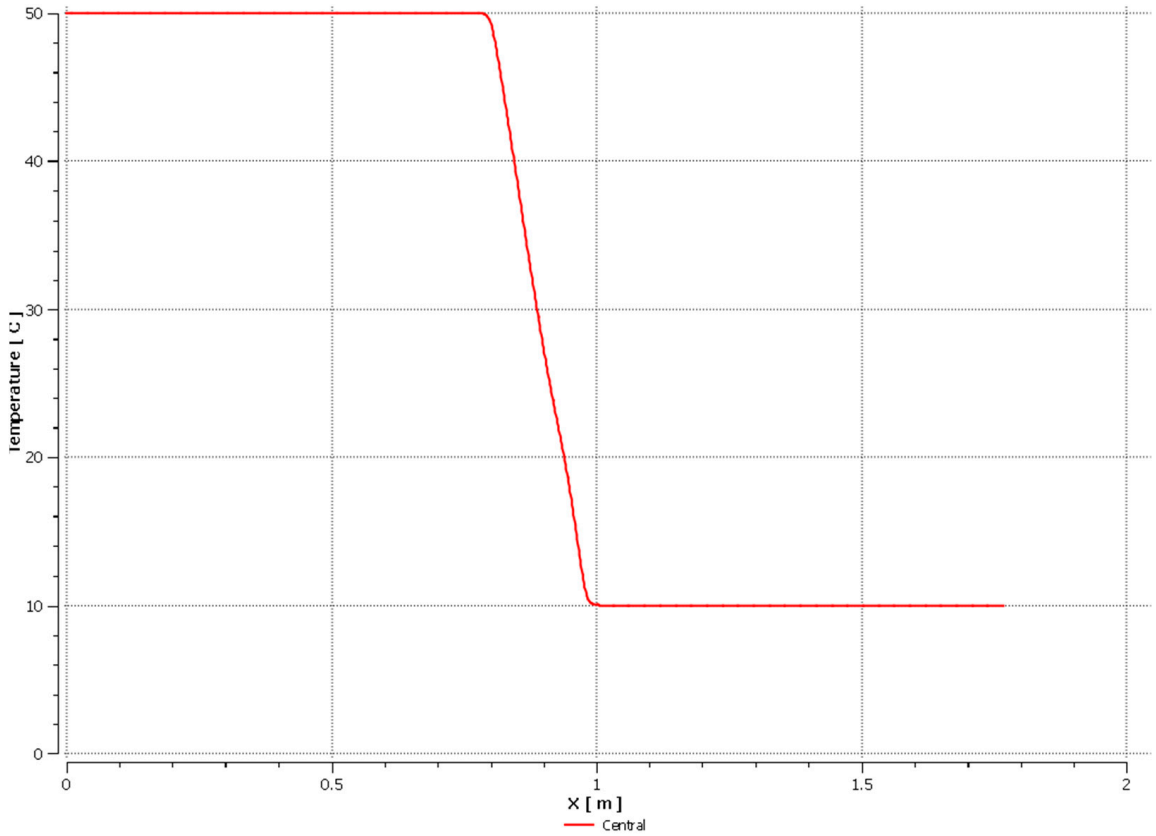

Figure 4. Temperature distribution along the height of the heat pipe's central line.

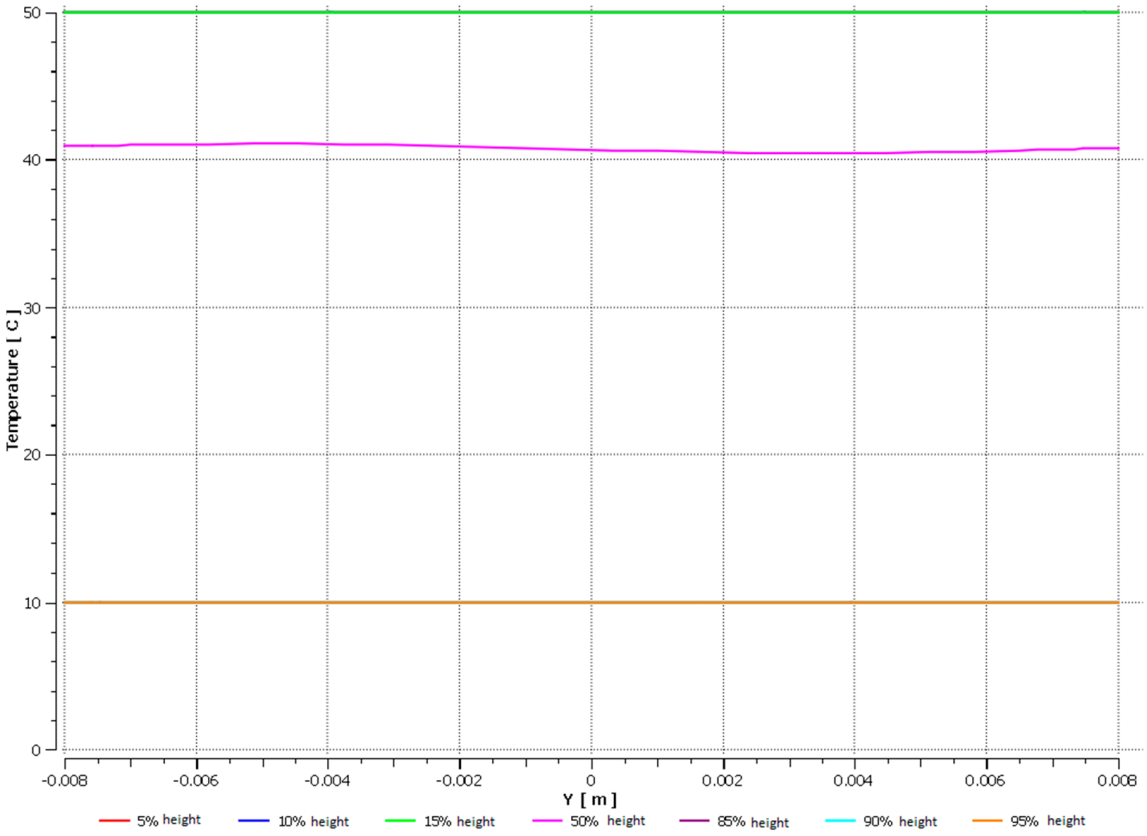

Figure 5. Temperature distribution along the cross-section.

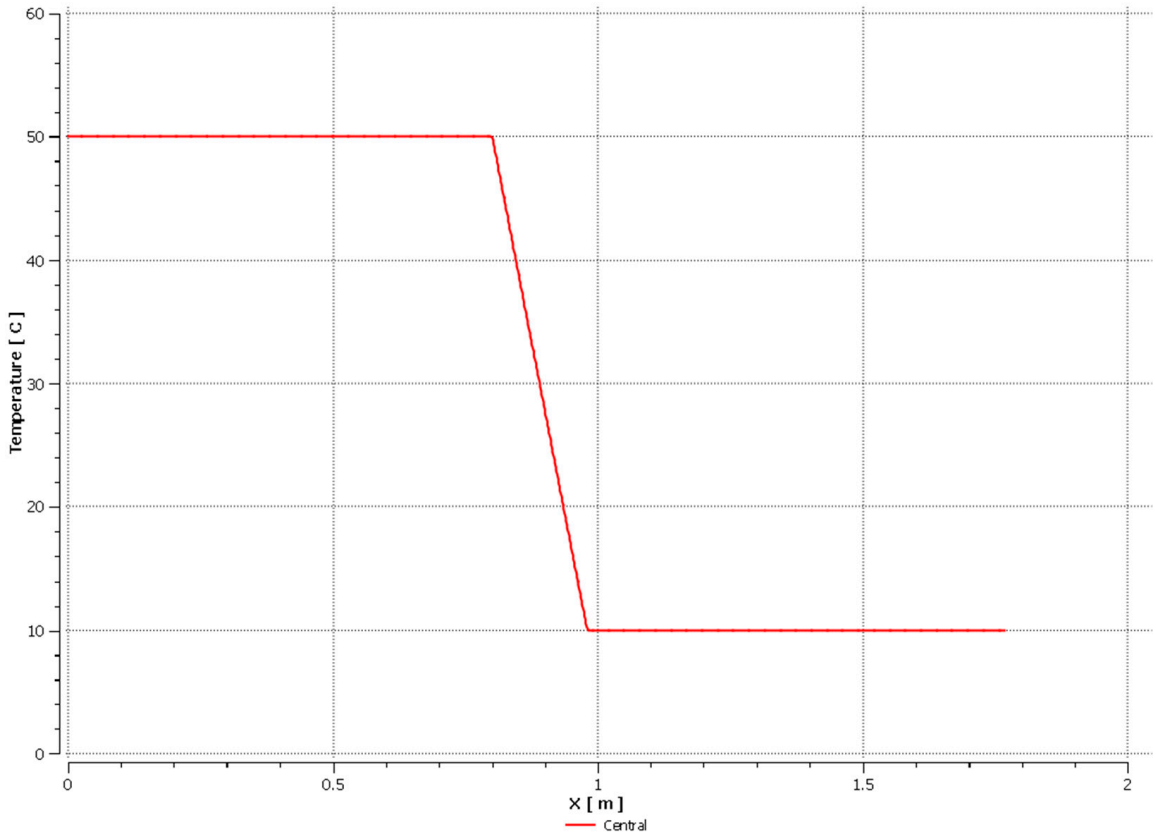

Figure 6. Temperature distribution along the height of the heat pipe's wall.

3.1.2. R134A Refrigerant-10% Filling of the Entire Volume of the Tube

The test results of the heat pipe with the R134A working medium in the filling amount of 10% of the total volume of the heat pipe proved heat transfer through the heat pipe. The differences in water temperatures at the inlet and outlet of the heat exchanger in the tested temperature range reached values from 1.59 °C to 11.60 °C.

The efficiency of the heat pipe for the tested filling was between 90% and 95%. The obtained simulation results indicate the point nature of the process of evaporation of the medium, i.e., this transformation does not take place evenly on the surface of the tube but mainly in the foci. This theory is supported by the local temperature changes on the pipe walls, as shown in Figures 7–11. As stated earlier, the phase changes are point-like, which is consistent with the actual behavior of fluids, where such a process usually takes place at sharp edges, for example, on scratches or processing residues on the tube. The reduced vapor content in the lower part of the device is also noteworthy, as shown in Figure 8. This indicates the correct operation of the device because the vapor condensation takes place in the upper part of the device, and in the lower part, the liquid is dominated by evaporation. This prevents unnecessary heat exchange at the hot liquid outlet in the lower part of the device, which can be observed in the case of other working media. This phenomenon is undesirable and reduces the efficiency of the apparatus. The very intense steam movement near the walls in the upper parts of the device, as shown in Figure 8, is also noteworthy. Along with the observable temperature changes of these walls, it is possible to state that an intense heat exchange takes place on their surface, and thus the phase change of the medium is visible. The intense heat exchange inside the tube is also evidenced by the vapor velocity profile, as shown in Figure 8, which indicates phase transitions on the surface of the inner walls of the tubes, and thus, the high value of the heat transfer coefficients.

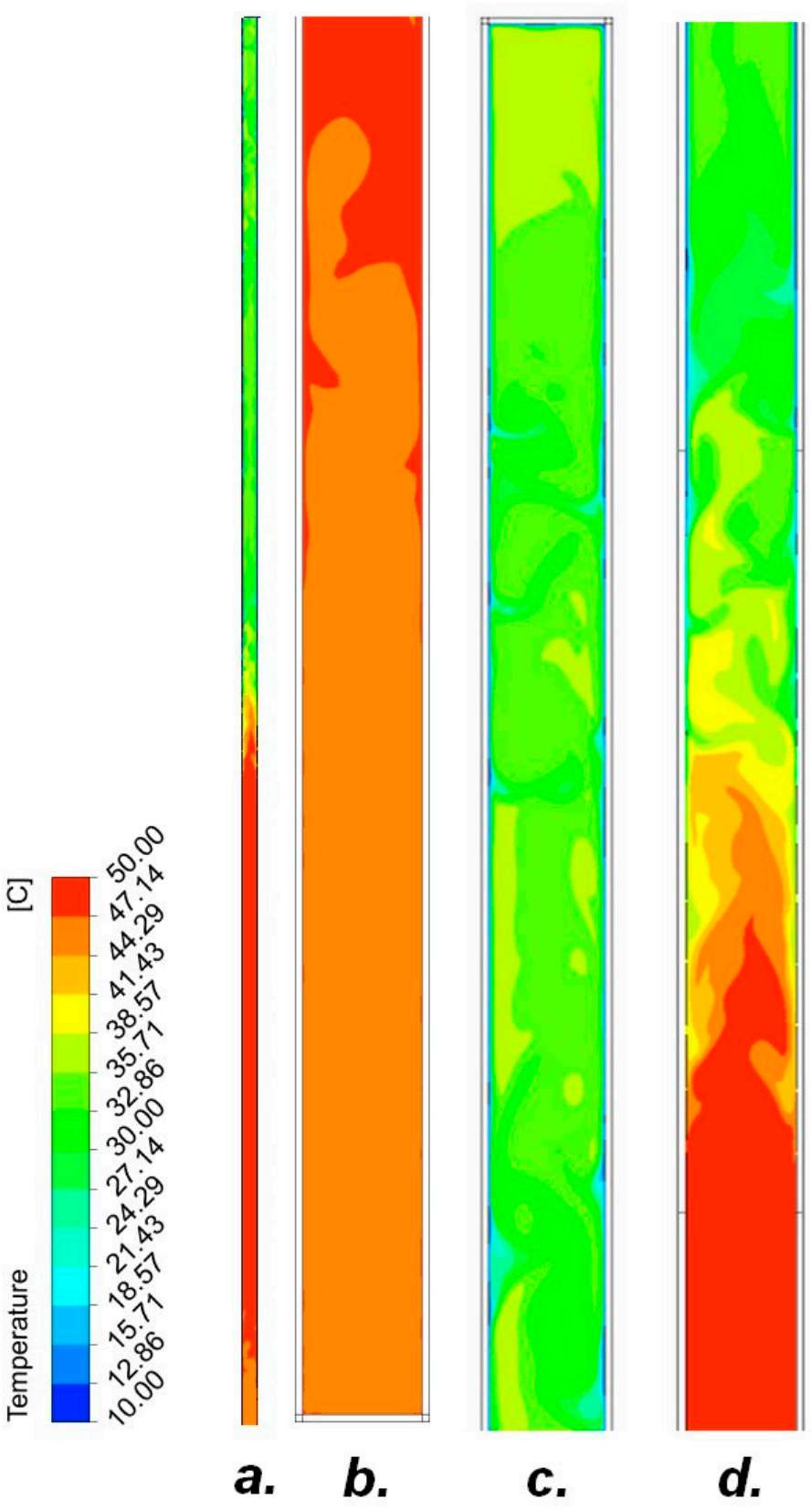

Figure 7. Temperature distribution in the heat pipe. (**a**) Total heat pipe; (**b**) evaporator section; (**c**) condenser section; (**d**) isothermal section.

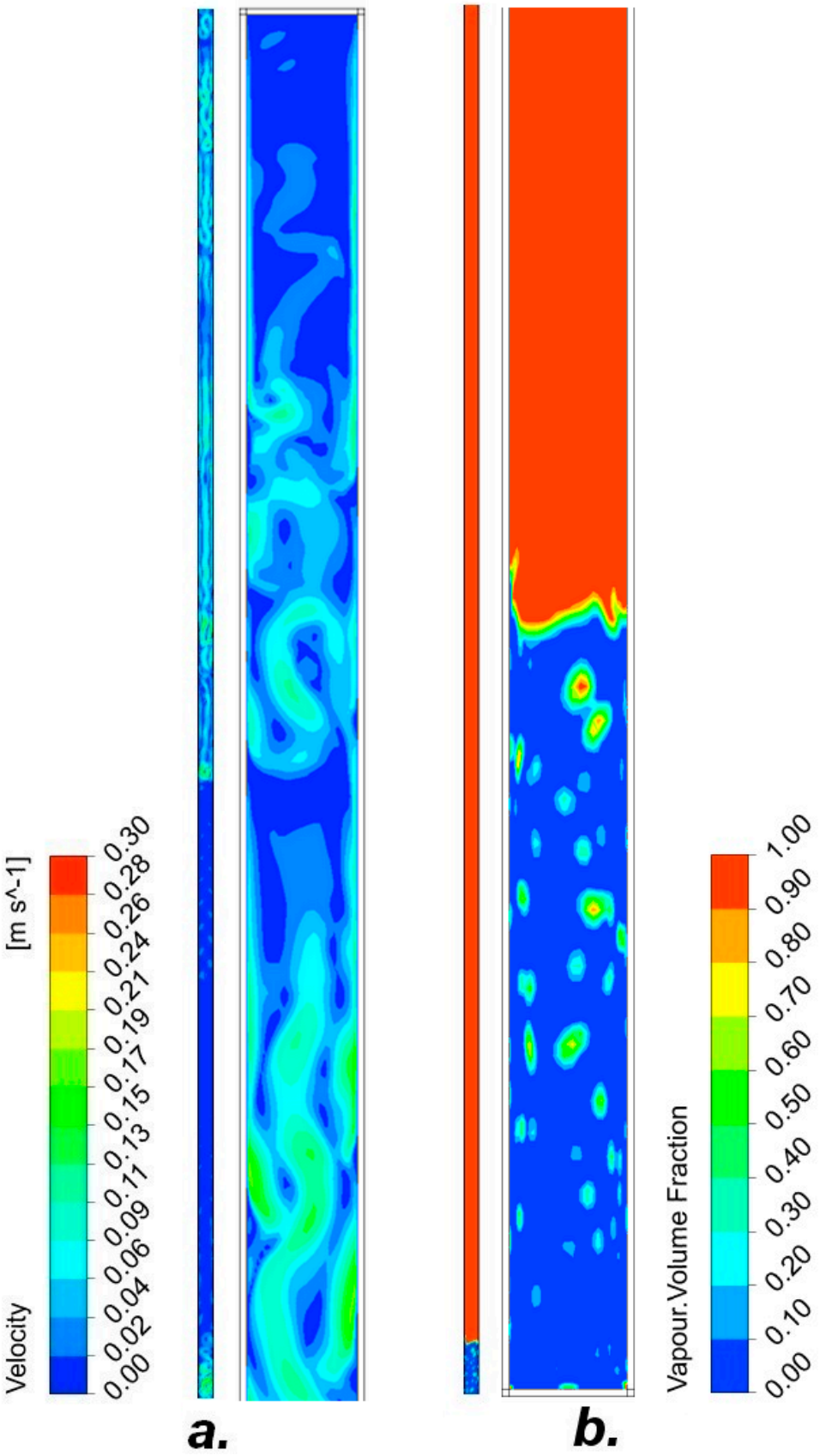

Figure 8. (**a**) Fluid velocity in the total heat pipe and in the condenser section, (**b**) the volume fraction of steam in the total heat pipe and in the evaporator section.

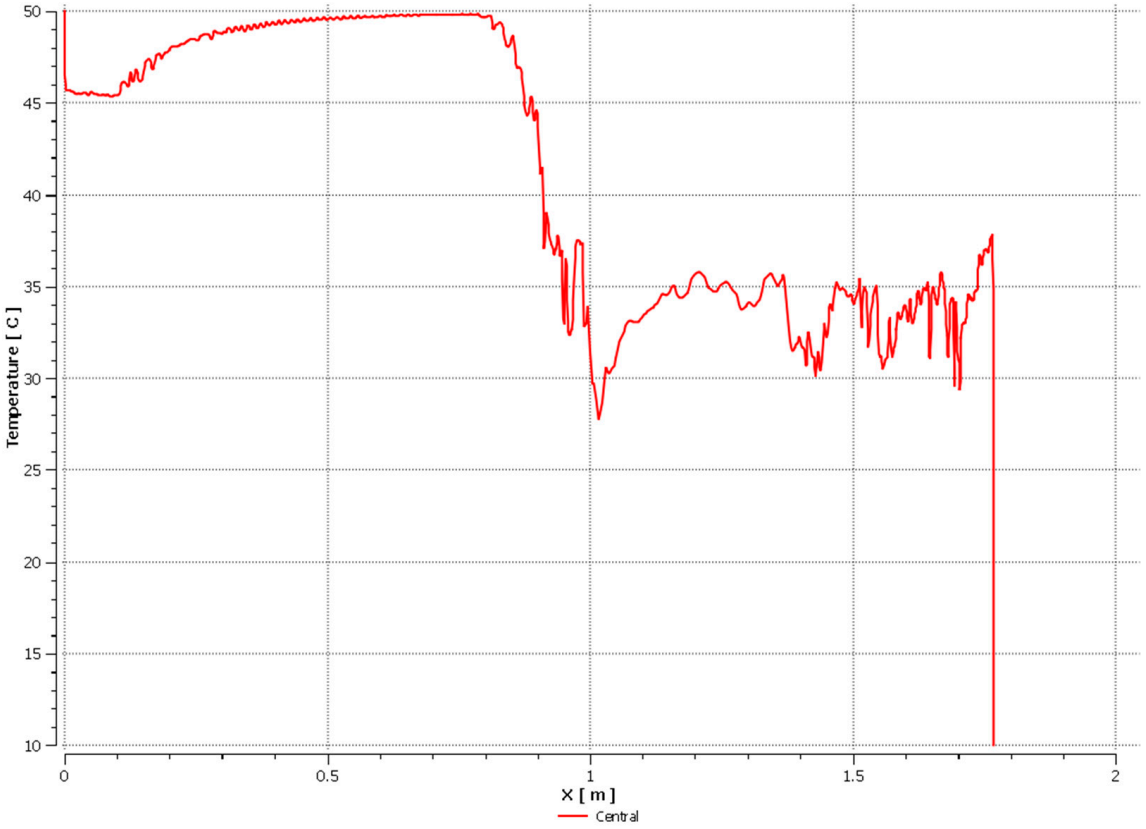

Figure 9. Temperature distribution along the height on the heat pipe's central line.

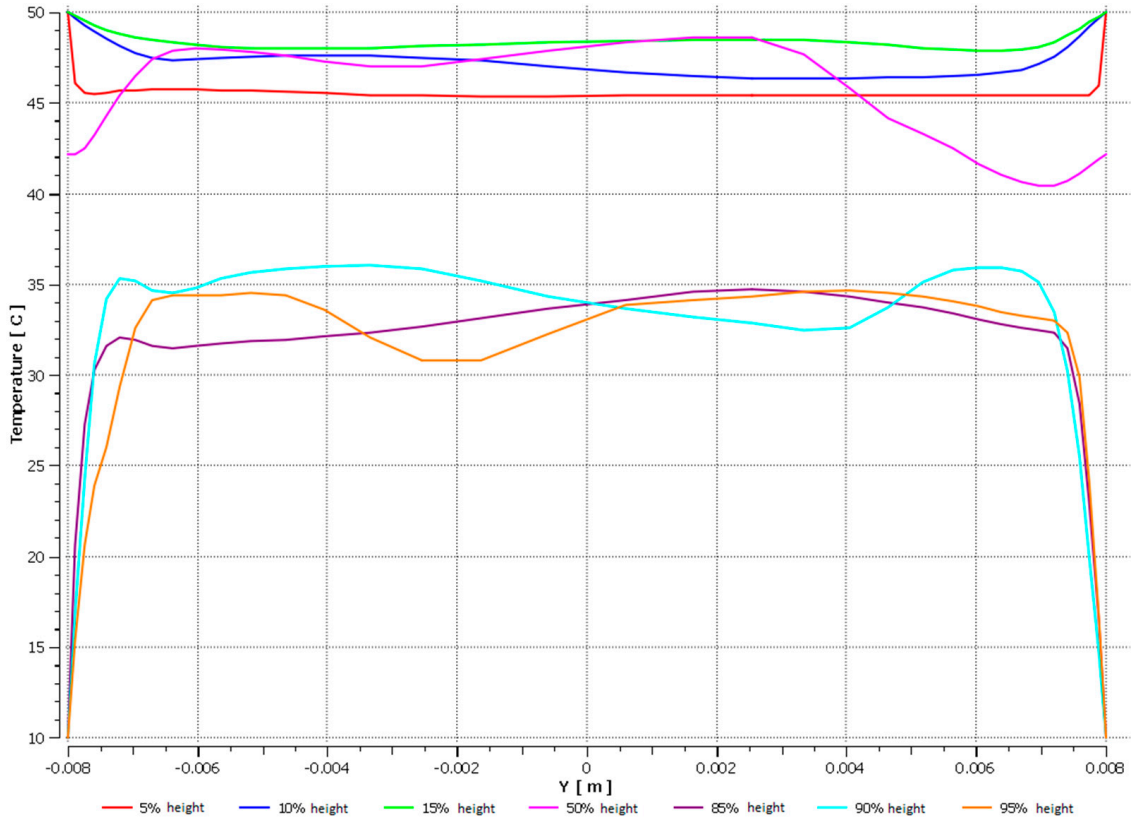

Figure 10. Temperature distribution along the cross-section.

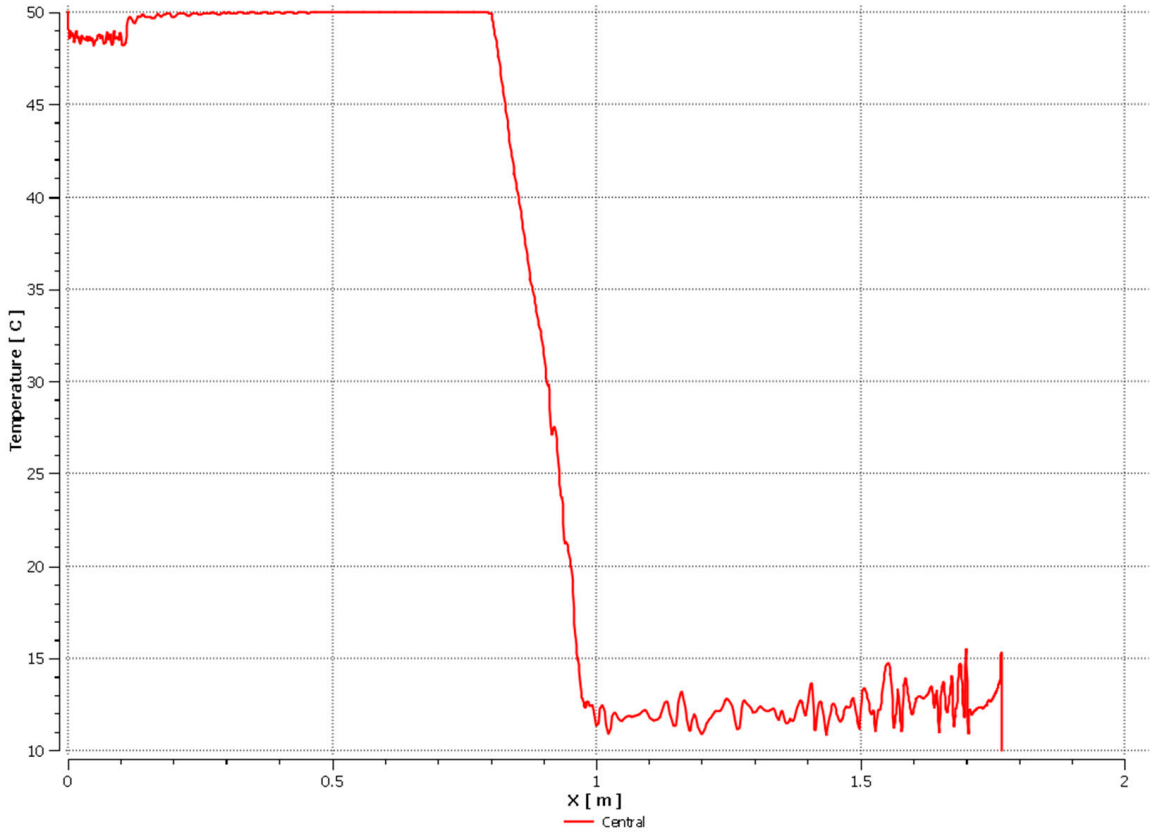

Figure 11. Temperature distribution along the height of the heat pipe's wall.

3.1.3. R404A-10% Filling of the Entire Tube Volume

The test results of the heat pipe with the working medium R404A in the filling amount of 10% of the total volume of the heat pipe proved heat transfer through the heat pipe. The differences in water temperatures at the inlet and outlet of the heat exchanger in the tested temperature range reached values from 1.15 °C to 10.21 °C. The efficiency of the heat pipe for the tested filling was between 83% and 92%.

The obtained results, shown in Figures 12–16, indicate that the behavior of the medium inside the tube is quite similar to that of the R134A medium. The differences are caused by the lower efficiency of the apparatus, but the mechanism of the processes taking place in it seems to be similar. They translate to the fact that the steam takes up a smaller part of the apparatus, as shown in Figure 13, and thus, the heat exchange in the lower part of the apparatus takes place on a much smaller part of it. This translates into a smaller area of his work. This is confirmed by the data presented in Figure 12; in a large part of both the lower and upper parts of the tube, the temperature of the medium is constant. This indicates that the heat transfer in this part of the apparatus is insignificant, which negatively affects the performance of the apparatus. The other graphs confirm that in these areas, the phase transitions are less intense than in the case of the R134A medium.

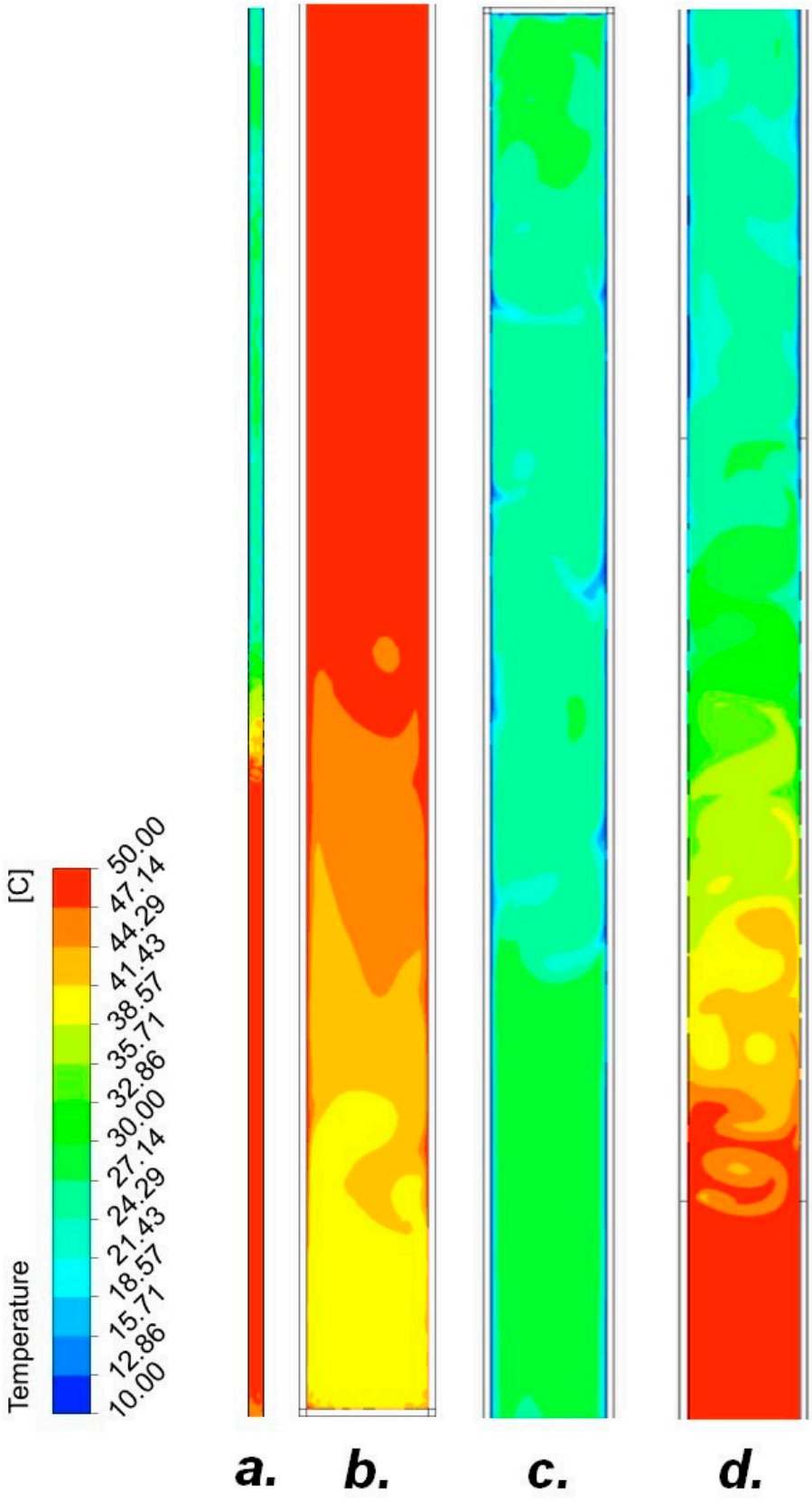

Figure 12. Temperature distribution in the heat pipe. (**a**) Total heat pipe; (**b**) evaporator section; (**c**) condenser section; (**d**) isothermal section.

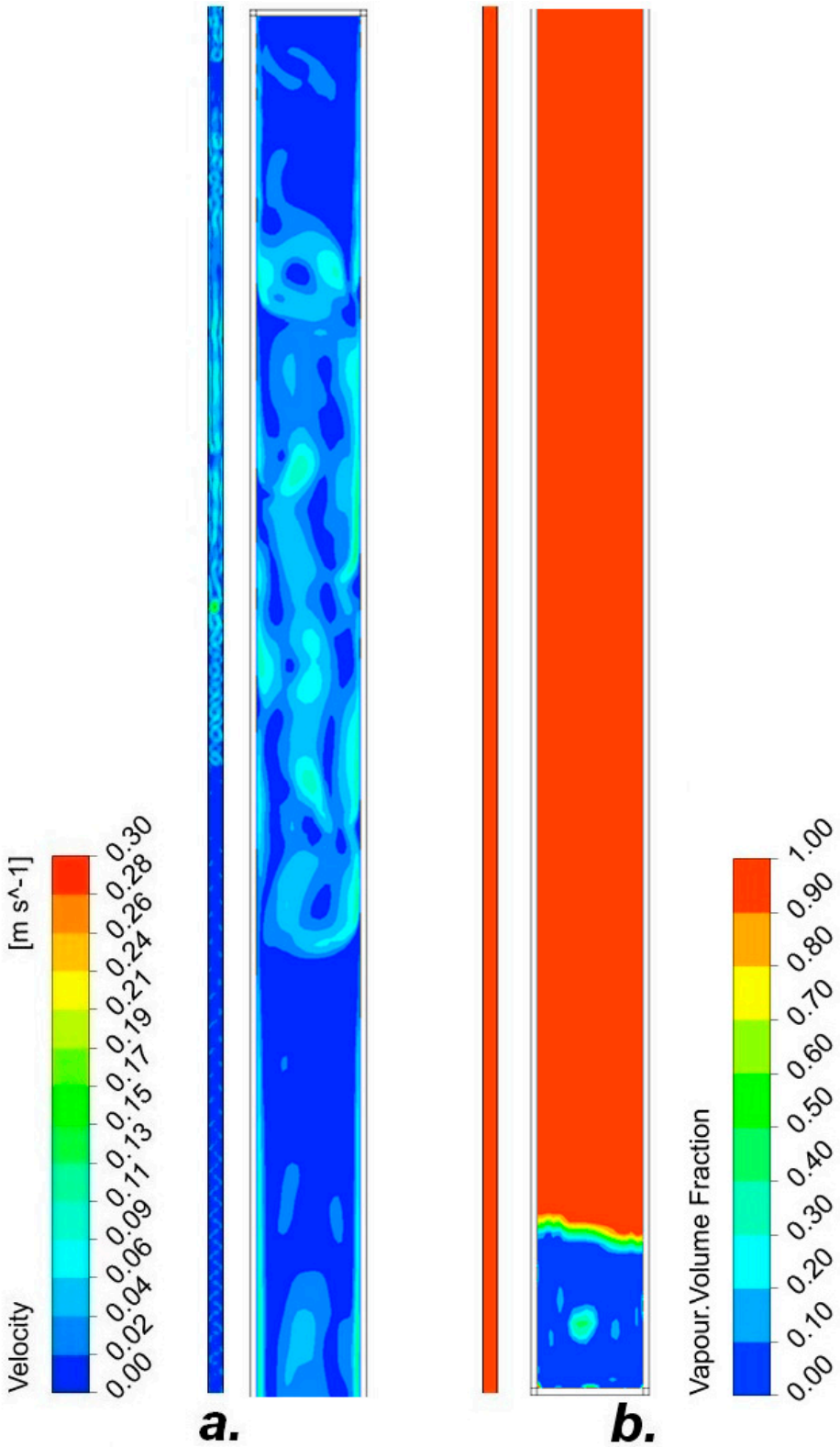

Figure 13. (**a**) Fluid velocity in the total heat pipe and in the condenser section. (**b**) The volume fraction of steam in the total heat pipe and in the evaporator section.

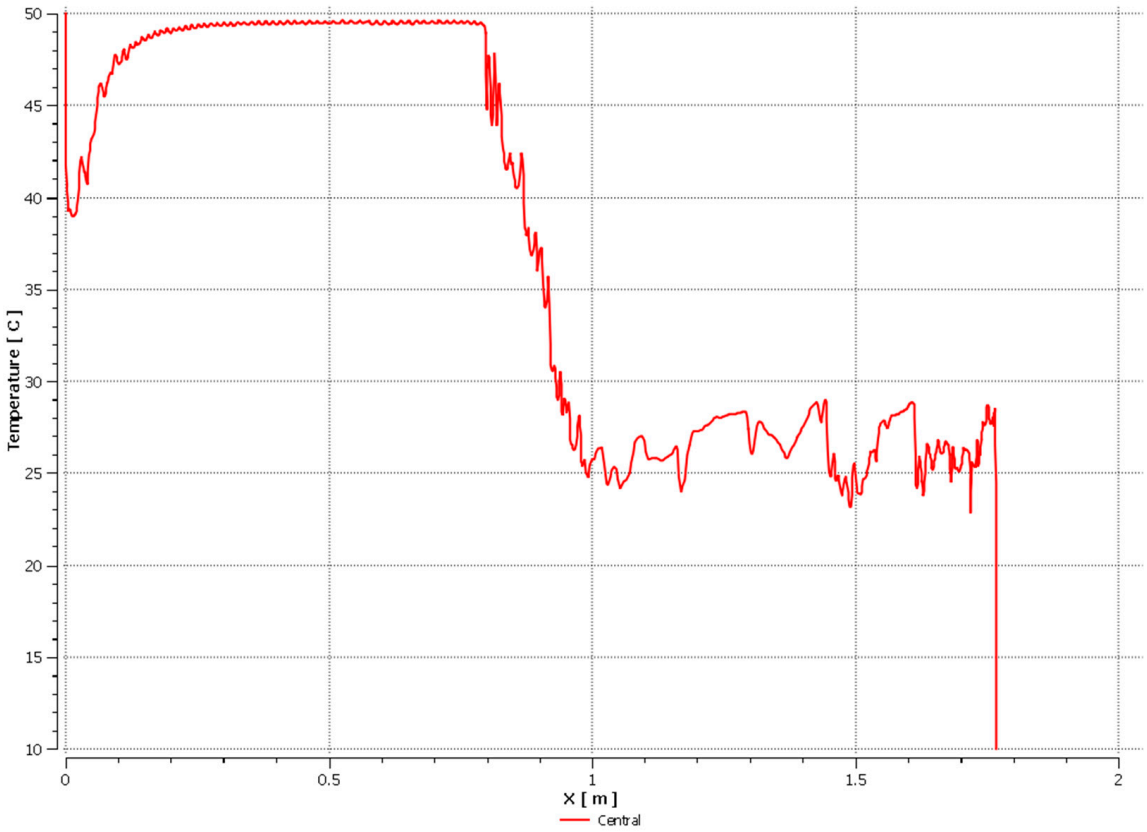

Figure 14. Temperature distribution along the height along the central line of the heat pipe.

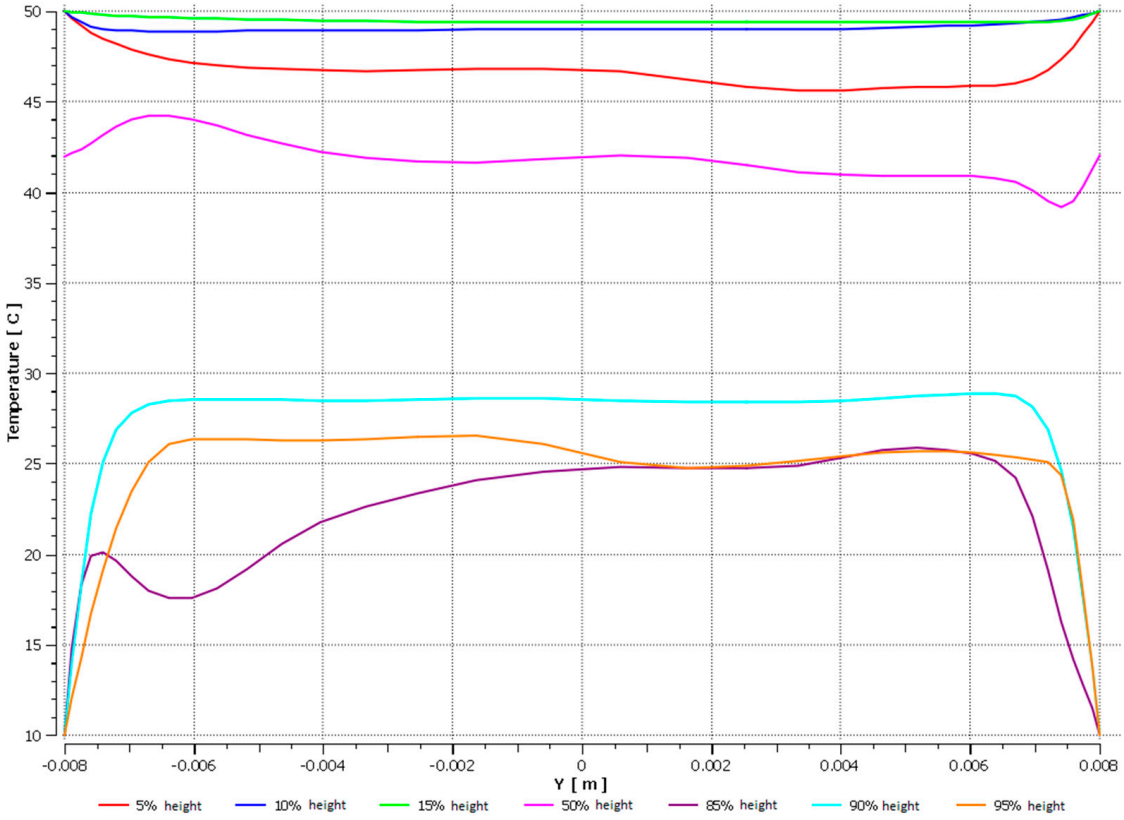

Figure 15. Temperature distribution along the cross-section.

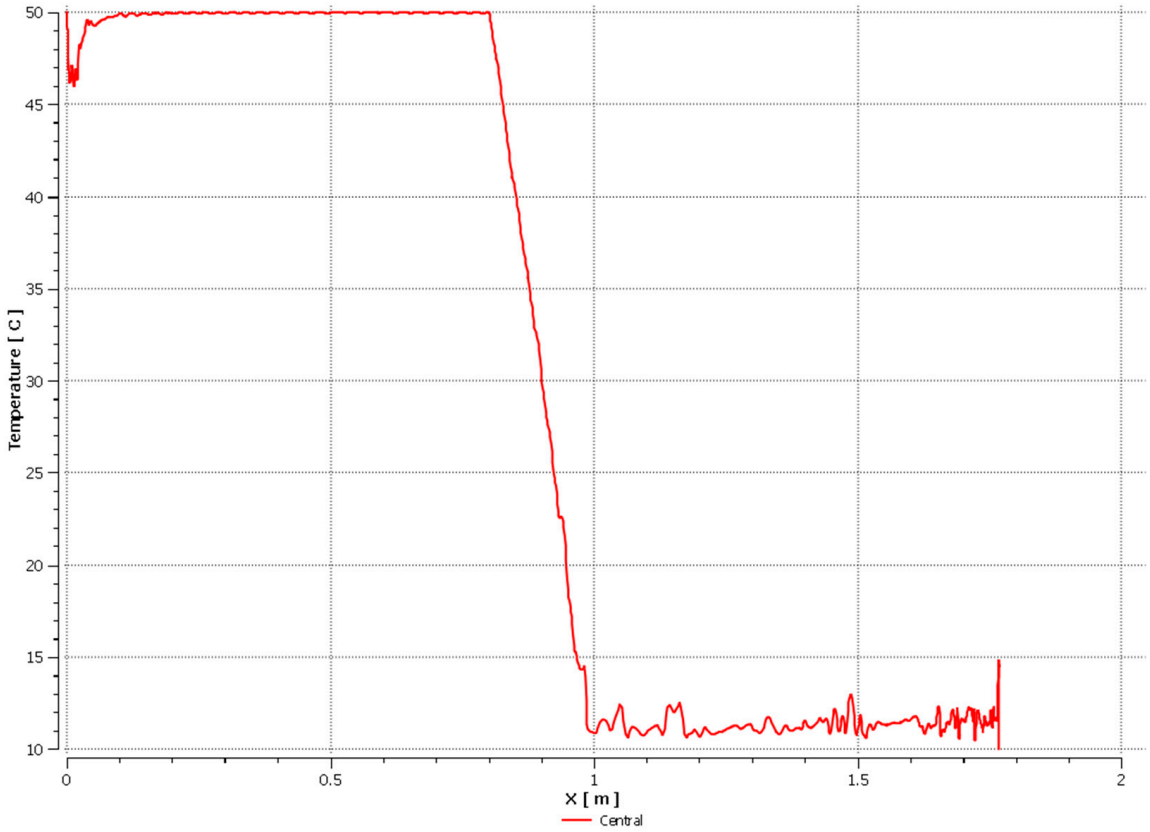

Figure 16. Temperature distribution along the height of the heat pipe's wall.

3.1.4. R407C-5% Filling of the Entire Tube Volume

The test results of the heat pipe with the R407C working medium in the filling amount of 5% of the total volume of the heat pipe proved heat transfer through the heat pipe. The differences in water temperatures at the inlet and outlet of the heat exchanger in the tested temperature range reached values from 0 °C to 9.46 °C. The efficiency of the heat pipe for the tested filling ranges from 0% to 78%. The tested medium is less effective than the previous one. In its case, it can be observed that the heat transfer is more uneven inside the lower part of the apparatus, as evidenced by a very uneven distribution of temperatures both inside the device and on its walls, as shown in Figures 17–21. On the other hand, the heat exchange in the upper part of the device is weaker, so that the processes related to the phase changes take place less intensively. For this reason, the reaction potential, which is the driving mechanism of the heat exchange inside the apparatus, is limited. Another limitation that can be observed is a very small volume of liquid in the lower part of the device. The steam occupies a large part of the lower half of the device, as shown in Figure 18. For this reason, in this part of the device, no intensive evaporation of the cooling liquid takes place, and therefore the heat from the heating water is absorbed by the medium only by convection. This translates into much lower effective heat transfer coefficients, and thus, low efficiency of the device. This is confirmed by the temperature distribution observed in Figures 19–21, where no significant changes in the temperature of the medium were observed in about 10% of the lower part of the device.

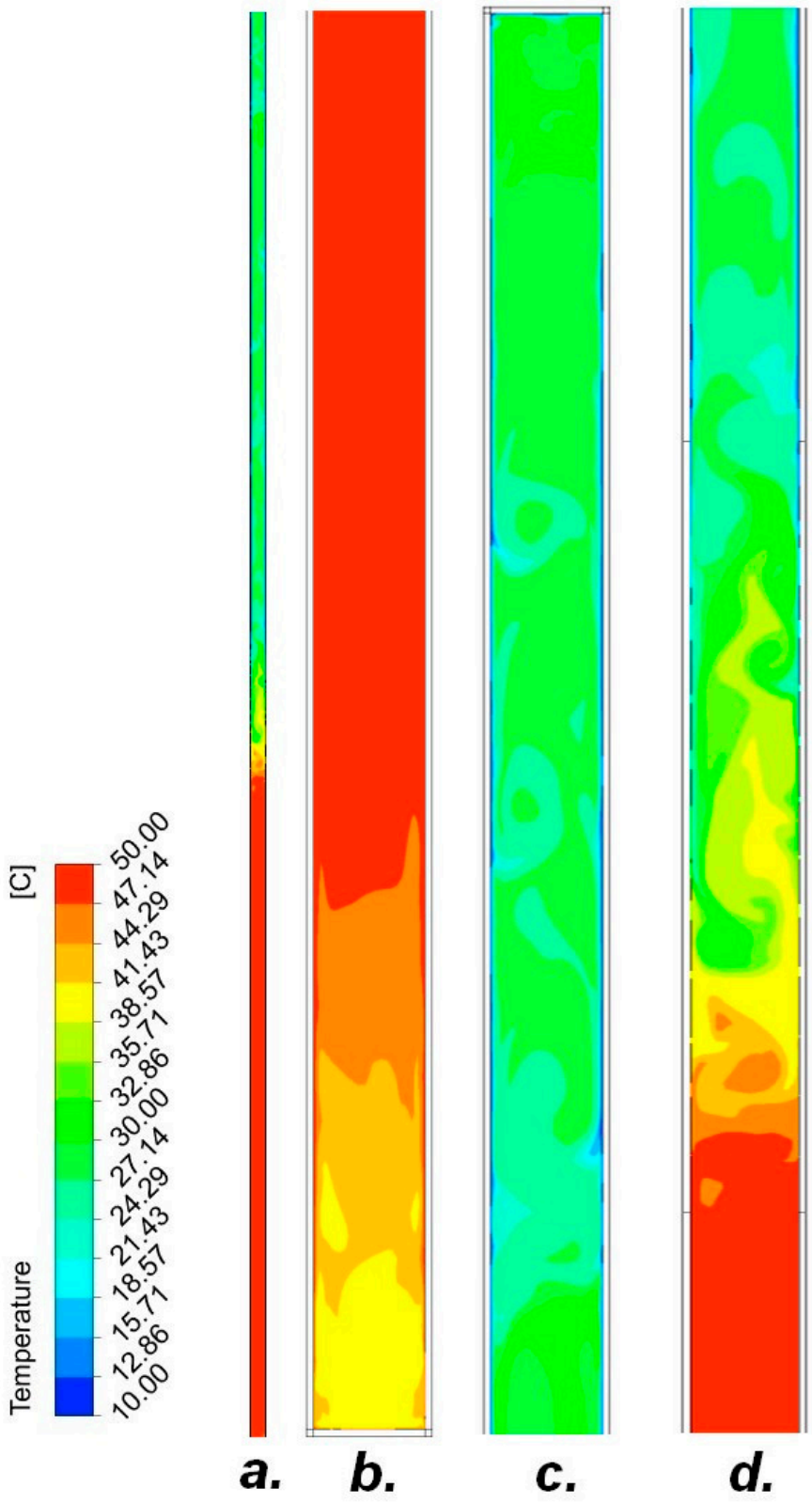

Figure 17. Temperature distribution in the heat pipe. (**a**) Total heat pipe; (**b**) evaporator section; (**c**) condenser section; (**d**) isothermal section.

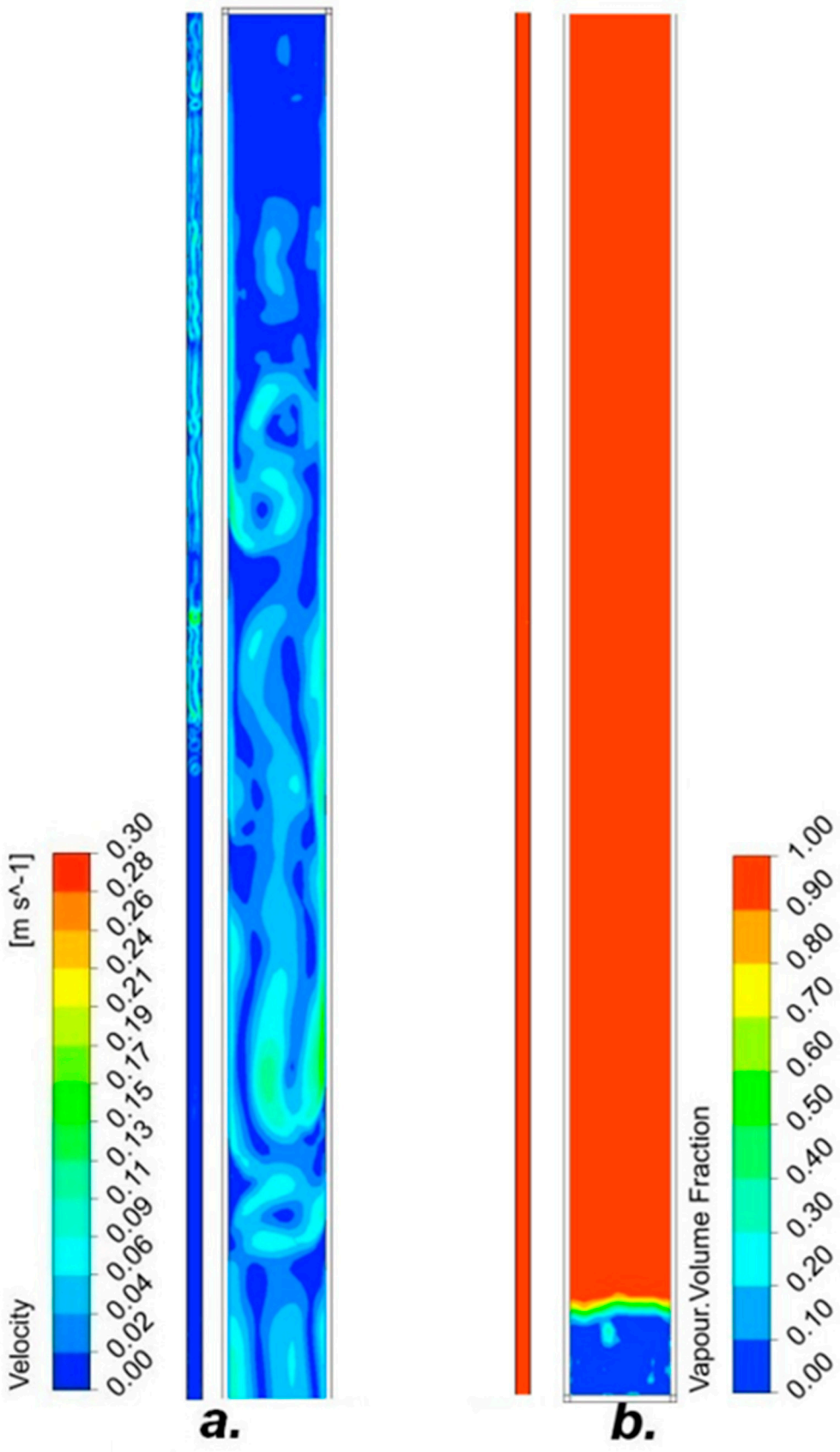

Figure 18. (**a**) Fluid velocity in the total heat pipe and in the condenser section, (**b**) the volume fraction of steam in the total heat pipe and in the evaporator section.

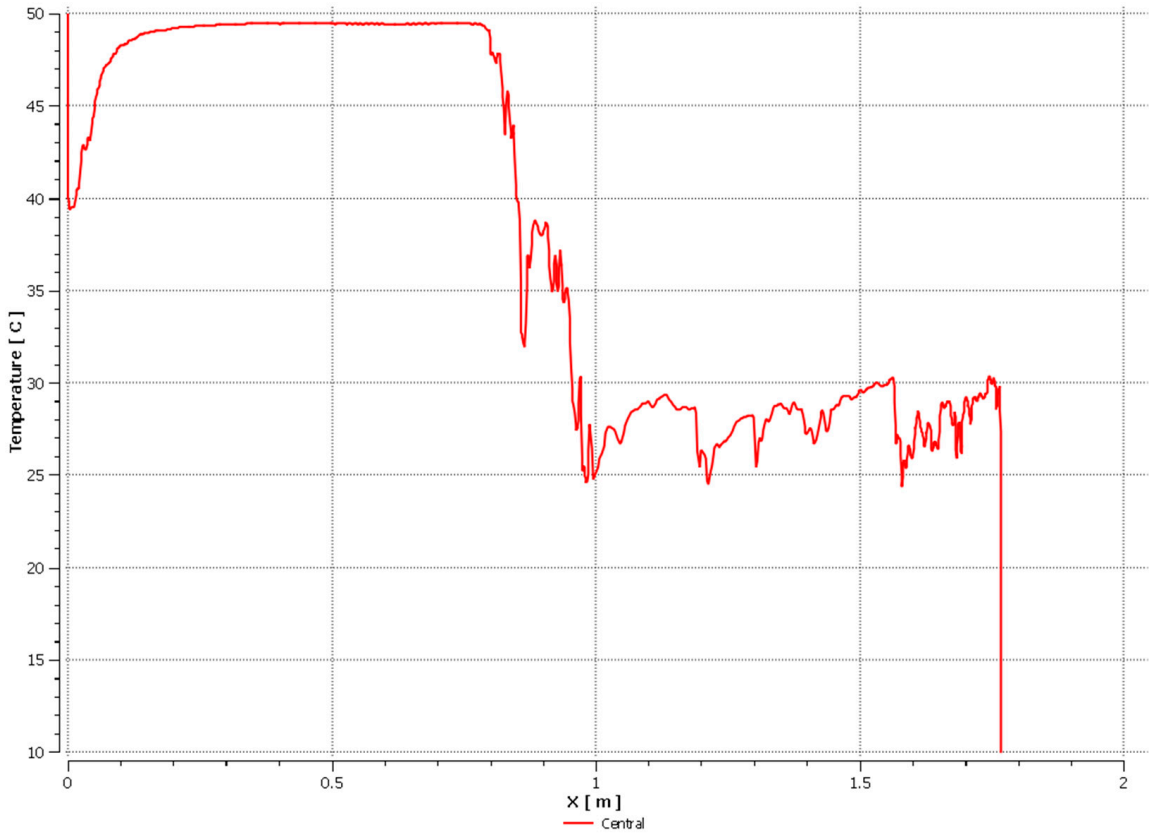

Figure 19. Temperature distribution along the height of the heat pipe's central line.

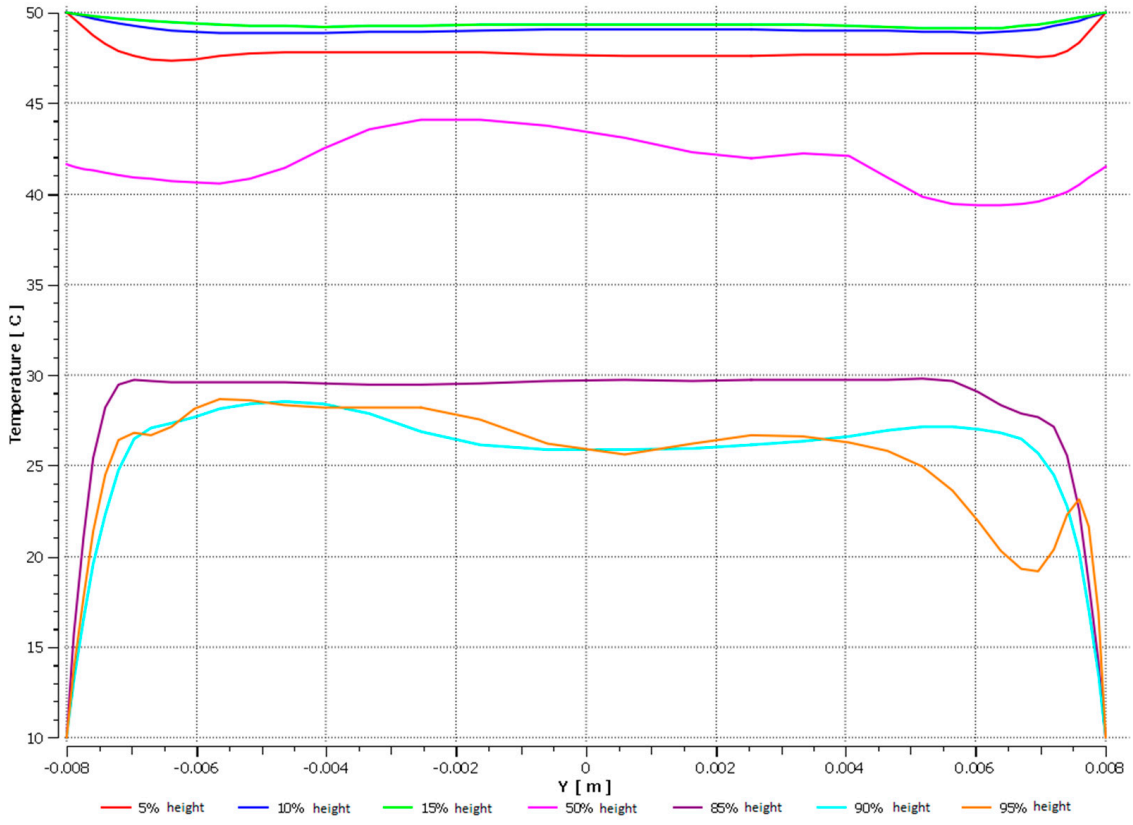

Figure 20. Temperature distribution along the cross-section.

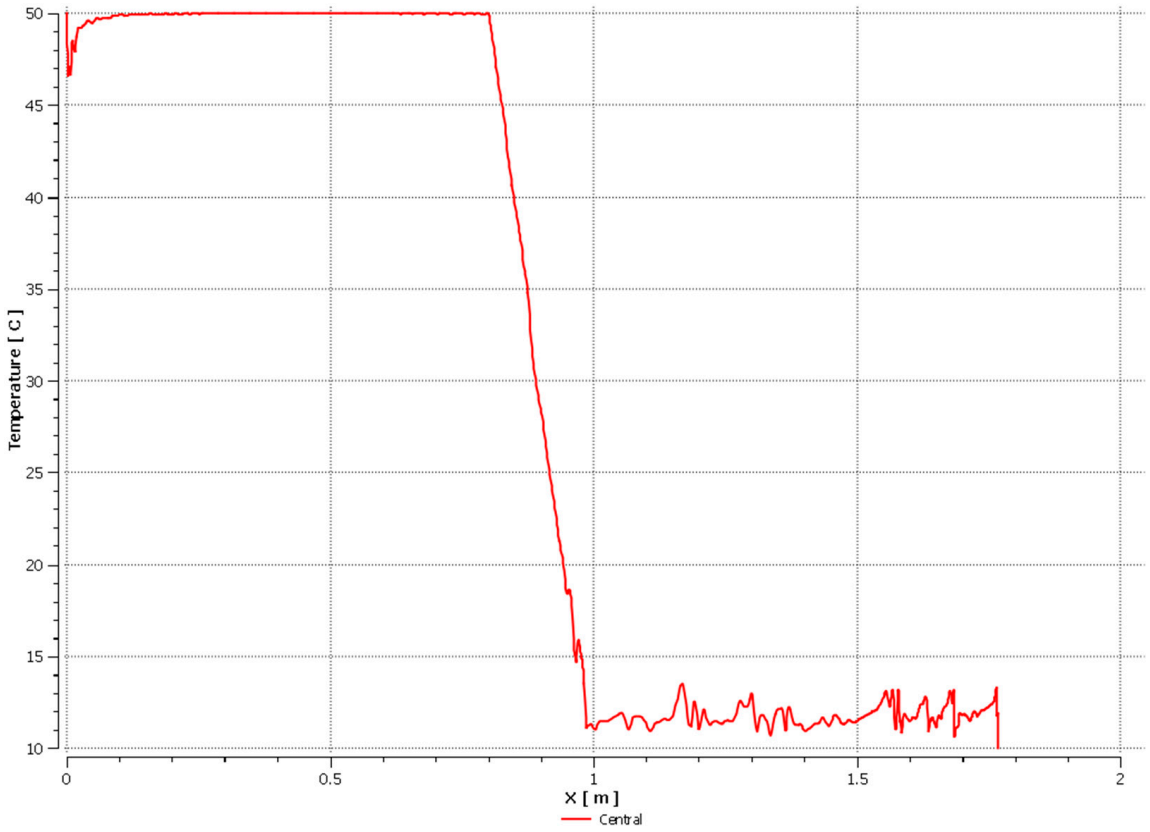

Figure 21. Temperature distribution along the height of the heat pipe's wall.

3.2. Pipe II

3.2.1. R134A-10% Filling of the Entire Tube Volume

When the heat pipe was filled with the R134A refrigerant in 10% of the volume, the highest values of heat flux collected by the evaporator and given off by the condenser (up to 130 W) were obtained. The heat pipe efficiency values for this filling were also high, ranging from 92% to 98%. Intensive heat exchange took place on the walls of the hot part of the apparatus. The graph describing the temperature distribution in the heat pipe (Figure 22) and the velocity profile (Figure 23) indicates the local turbulence of the flow, as well as the intense processes of phase changes, which make it possible to conclude about high values of the heat transfer coefficients. Moreover, both the wall temperature profiles and the wall vapor velocity profiles indicate intense phase changes in both the hot and cold parts of the apparatus. The shape of the temperature graph in the middle of the heat pipe is also noteworthy (Figure 24). As you can see, in contrast to the previously described cases, one can observe intense heat exchange in this part; the heat exchange takes place almost abruptly between the upper and lower part of the device (Figures 25 and 26). The graph shows that there are no mass transfer dead zones that could be observed for the R404A and R407C media. This indicates a very high efficiency of the device-heat exchange processes takes place in almost the entire volume of the system.

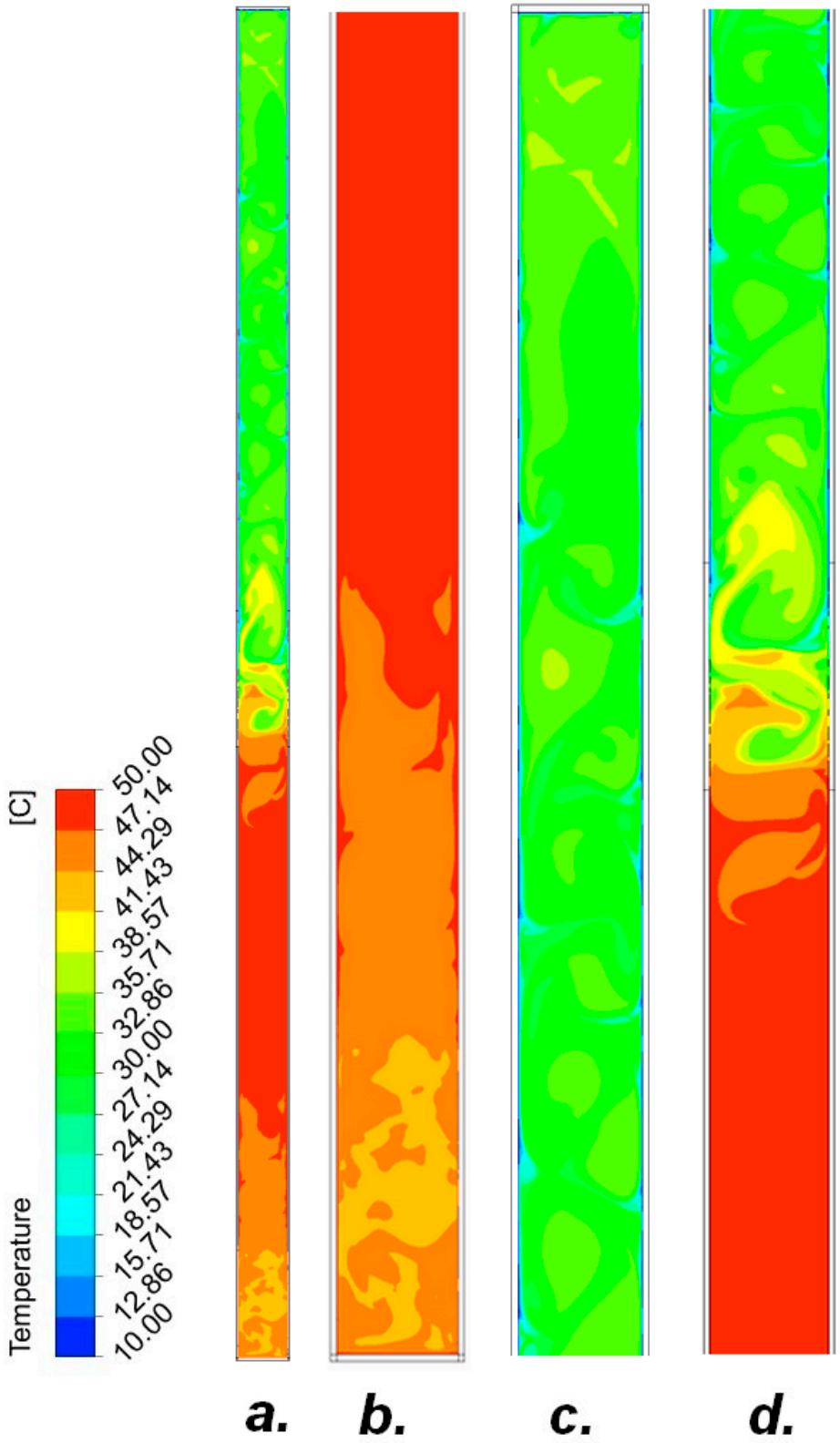

Figure 22. Temperature distribution in the heat pipe. (**a**) Total heat pipe; (**b**) evaporator section; (**c**) condenser section; (**d**) isothermal section.

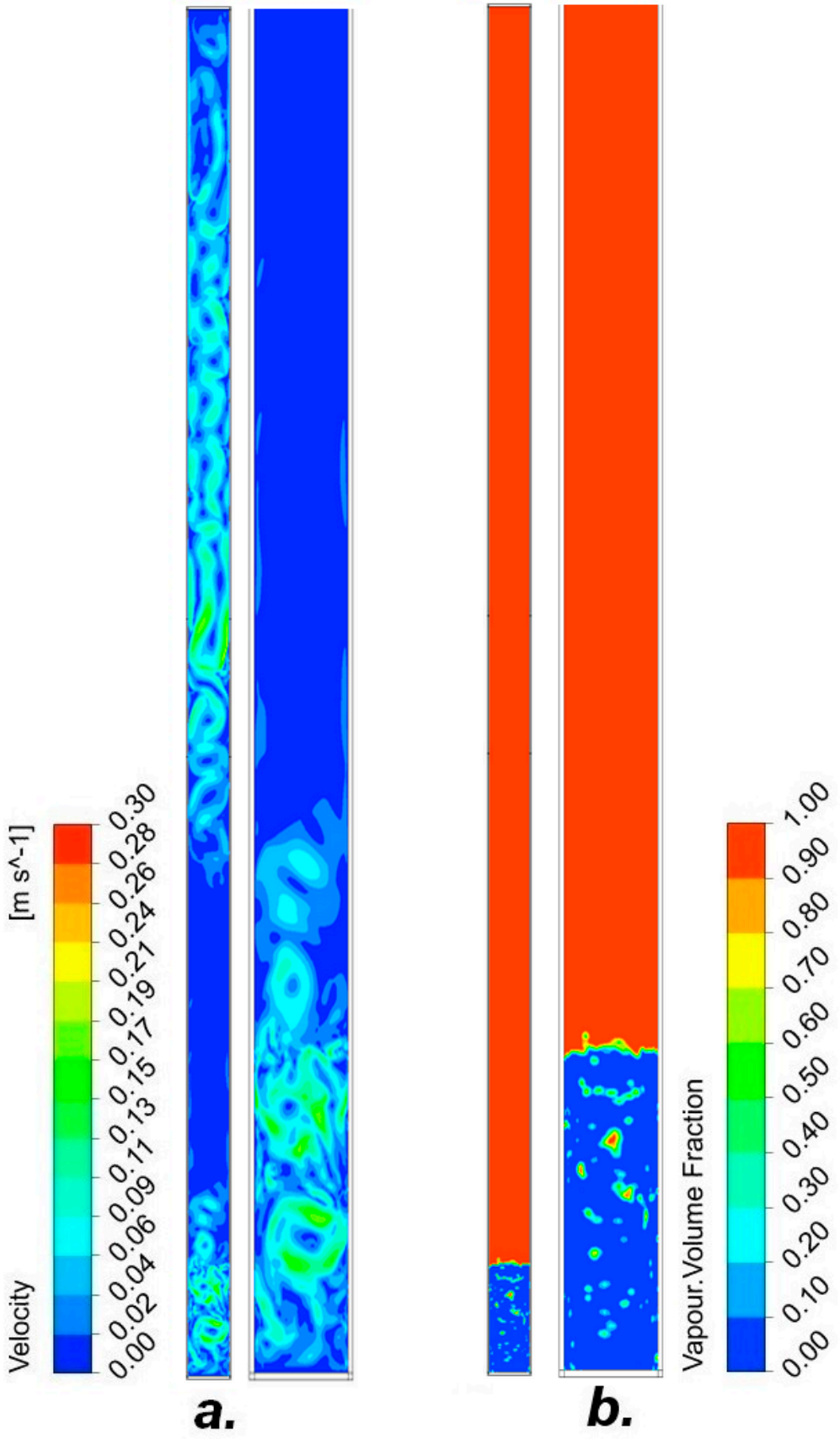

Figure 23. (**a**) Fluid velocity in the total heat pipe and in the condenser section, (**b**) the volume fraction of steam in the total heat pipe and in the evaporator section.

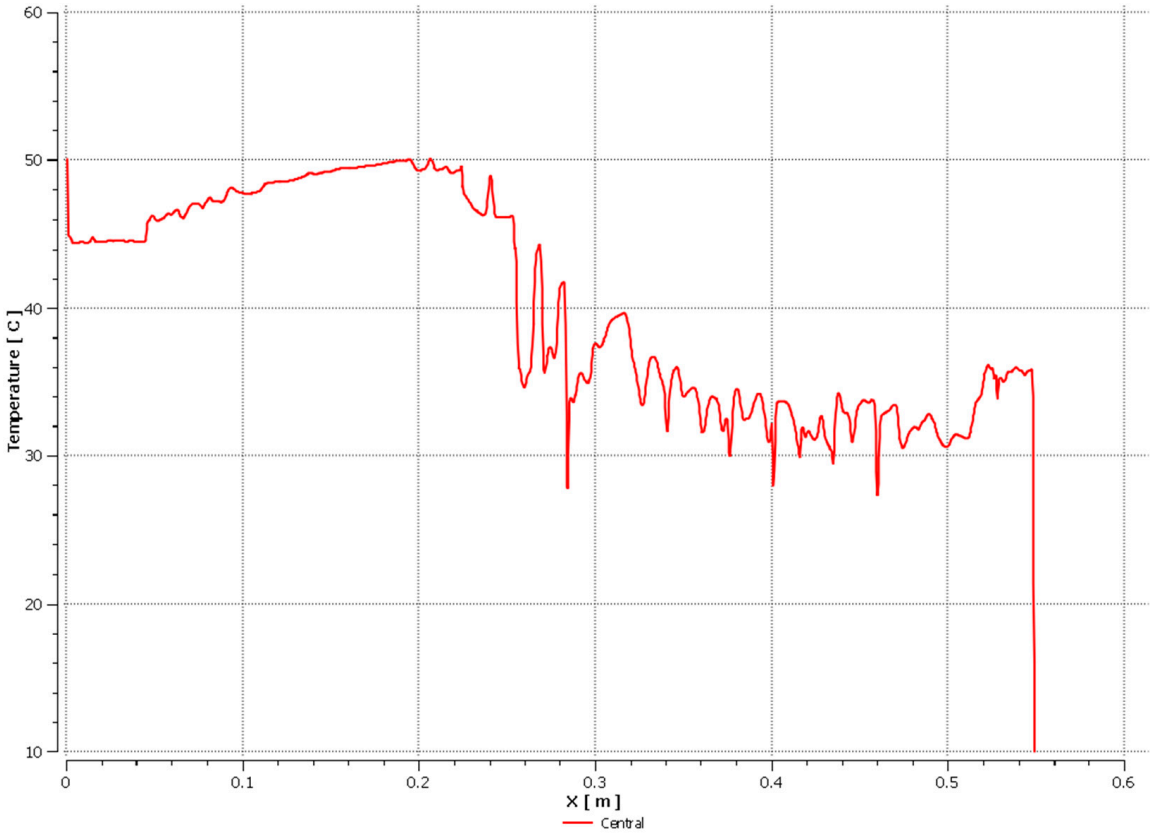

Figure 24. Temperature distribution along the height of the heat pipe's central line.

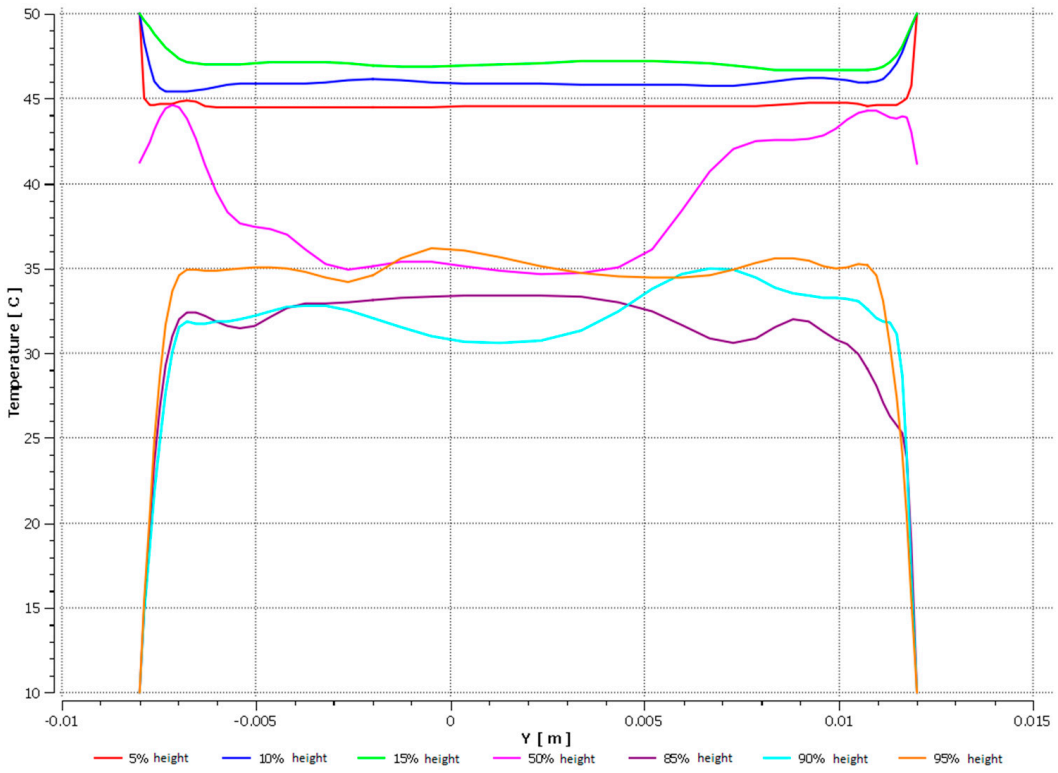

Figure 25. Temperature distribution along the cross-section.

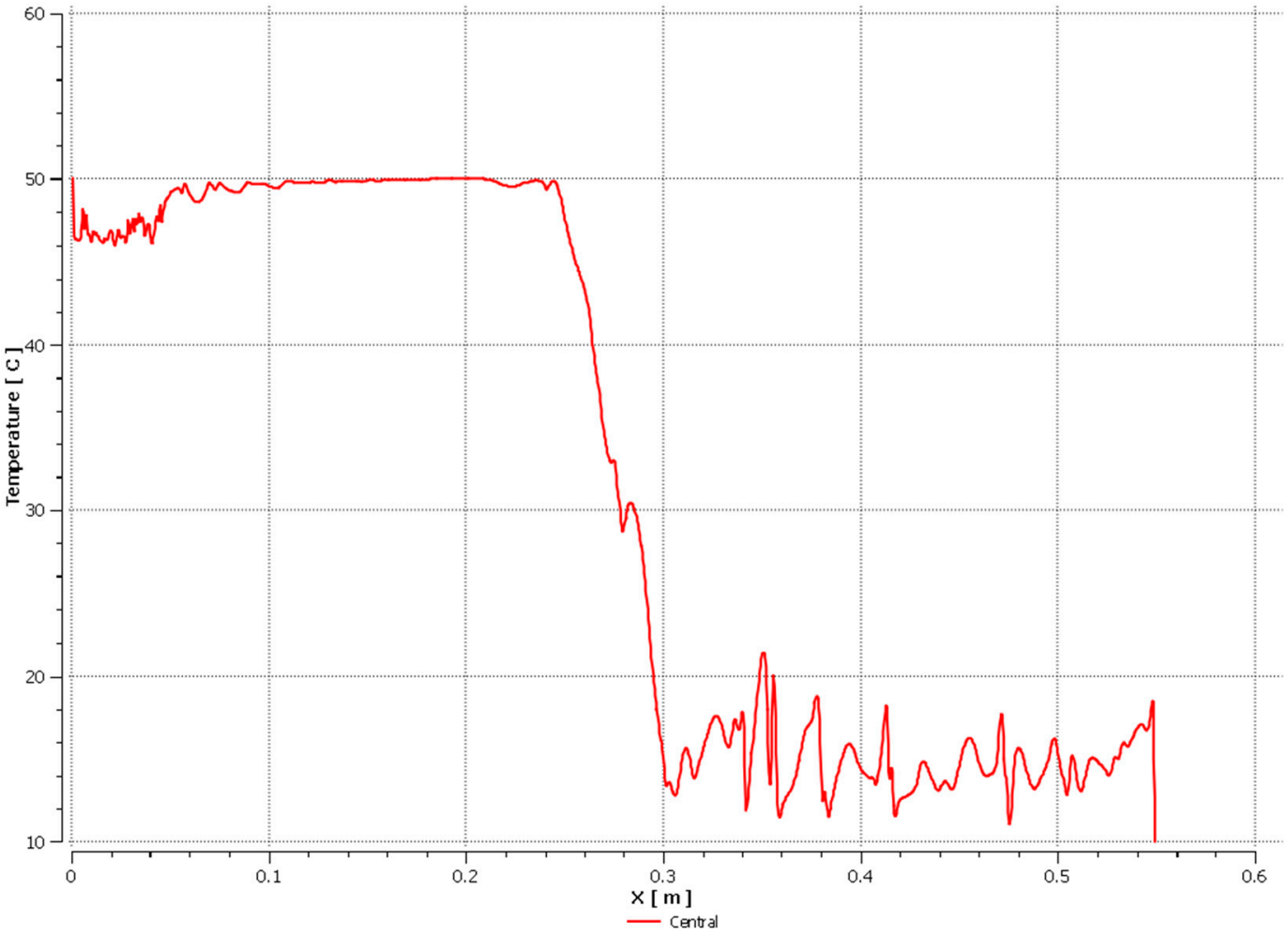

Figure 26. Temperature distribution along the height of the heat pipe's wall.

3.2.2. R404A-10% Fill the Entire Volume of the Tube

In most of the analyzed cases, the most effective working medium was R134A with 10% filling in the heat tube, followed by R404A also with 10% filling (Figures 27–31).

3.2.3. R407C-30% Filling of the Entire Tube Volume

R407C turned out to be the least effective factor among those tested. The heat pipe working with the R407C factor is characterized by low heat transport efficiency, low efficiency and the highest pressure values inside it during operation in a given temperature range (Figures 32–36). The results of computer simulations and calculations of the theoretical model correlated with the results on the test stand. The temperature distributions obtained as a result of computer simulations confirm the obtained experimental results.

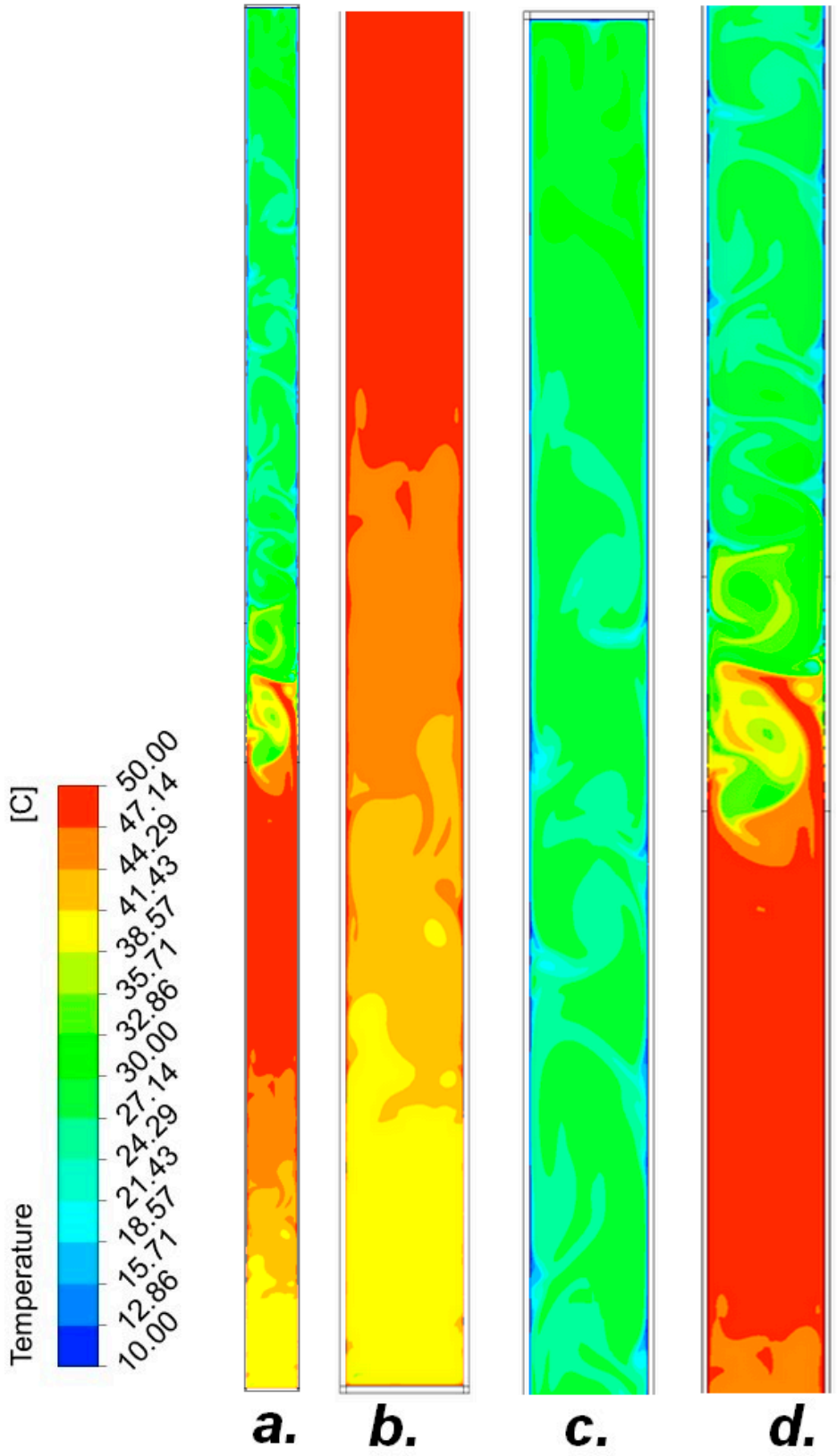

Figure 27. Temperature distribution in the heat pipe. (**a**) Total heat pipe; (**b**) evaporator section; (**c**) condenser section; (**d**) isothermal section.

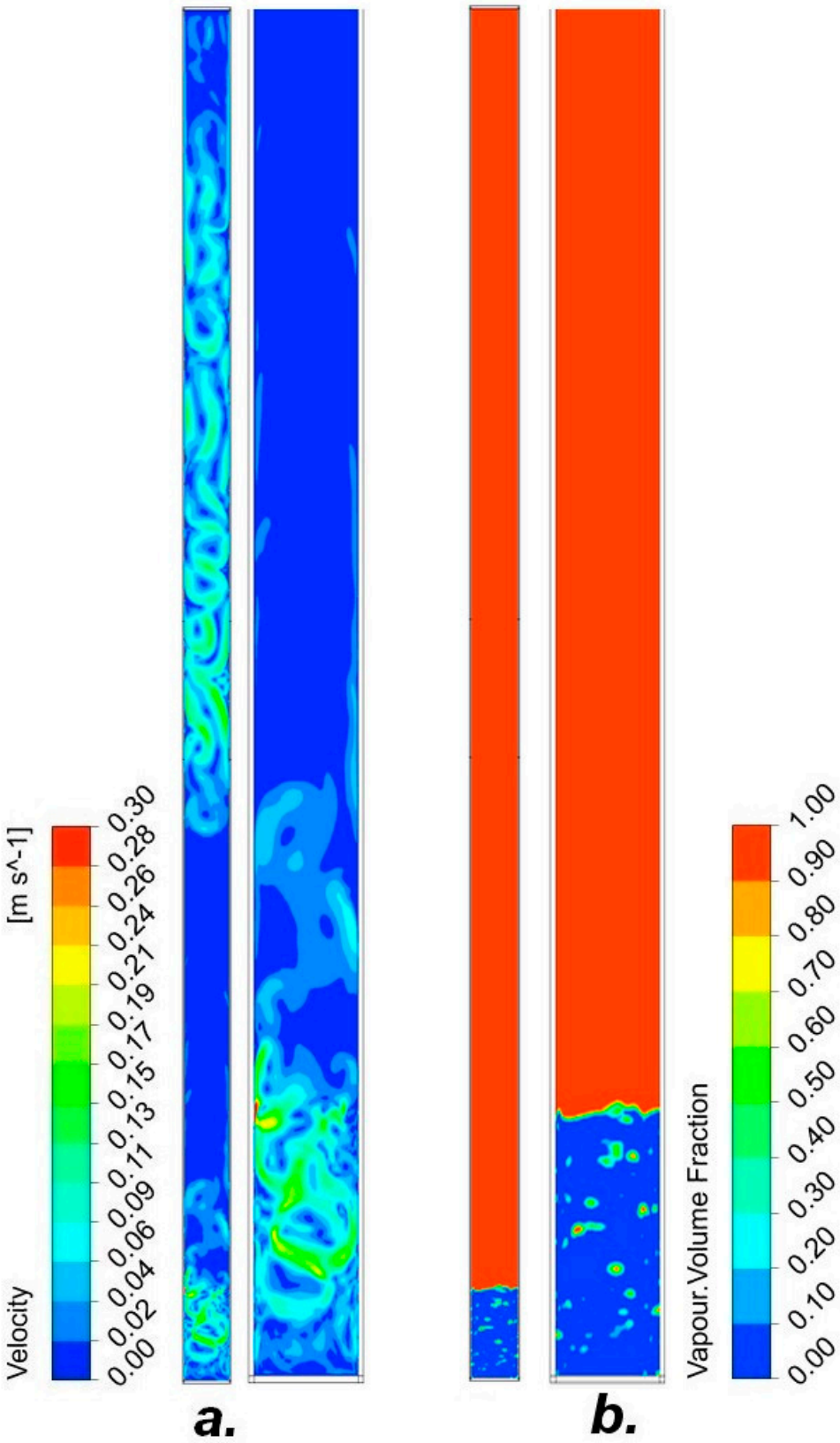

Figure 28. (**a**) Fluid velocity in the total heat pipe and in the condenser section, (**b**) the volume fraction of steam in the total heat pipe and in the evaporator section.

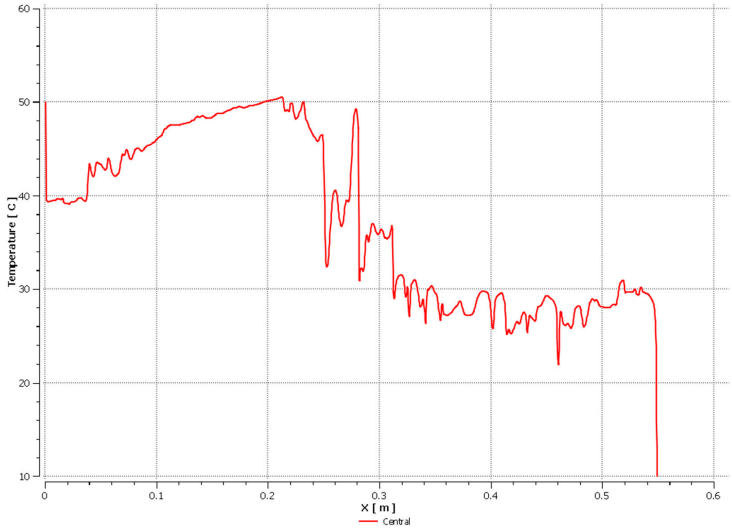

Figure 29. Temperature distribution along the height of the heat pipe's central line.

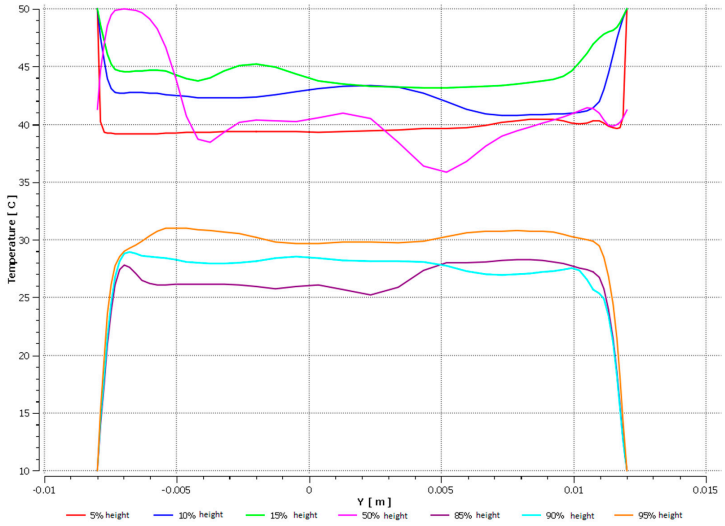

Figure 30. Temperature distribution along the cross-section.

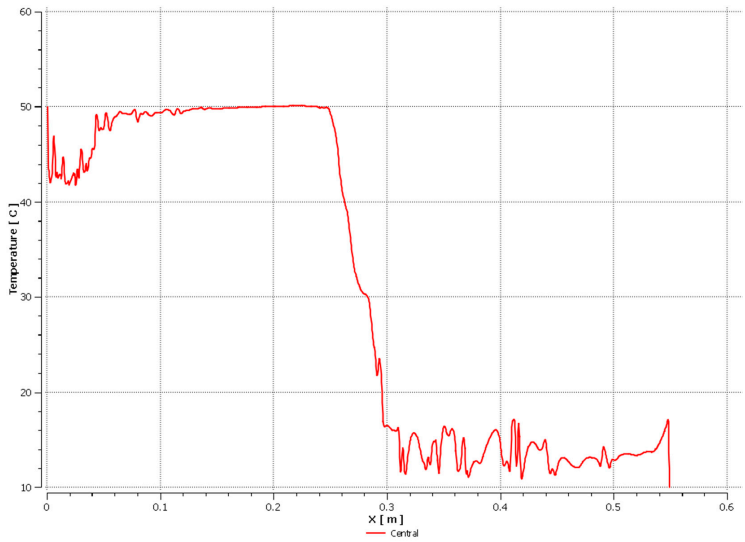

Figure 31. Temperature distribution along the height of the heat pipe's wall.

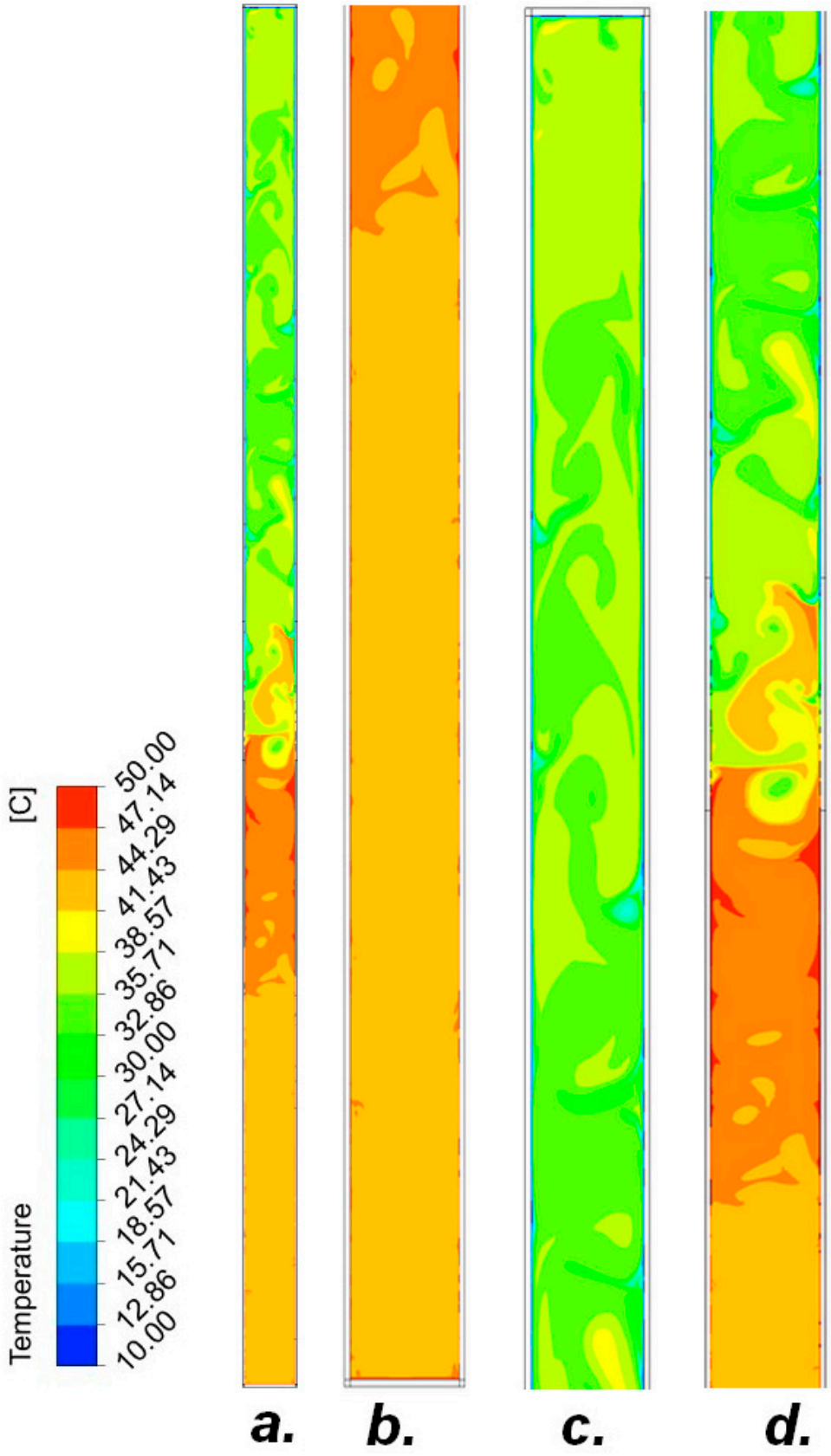

Figure 32. Temperature distribution in the heat pipe. (**a**) Total heat pipe; (**b**) evaporator section; (**c**) condenser section; (**d**) isothermal section.

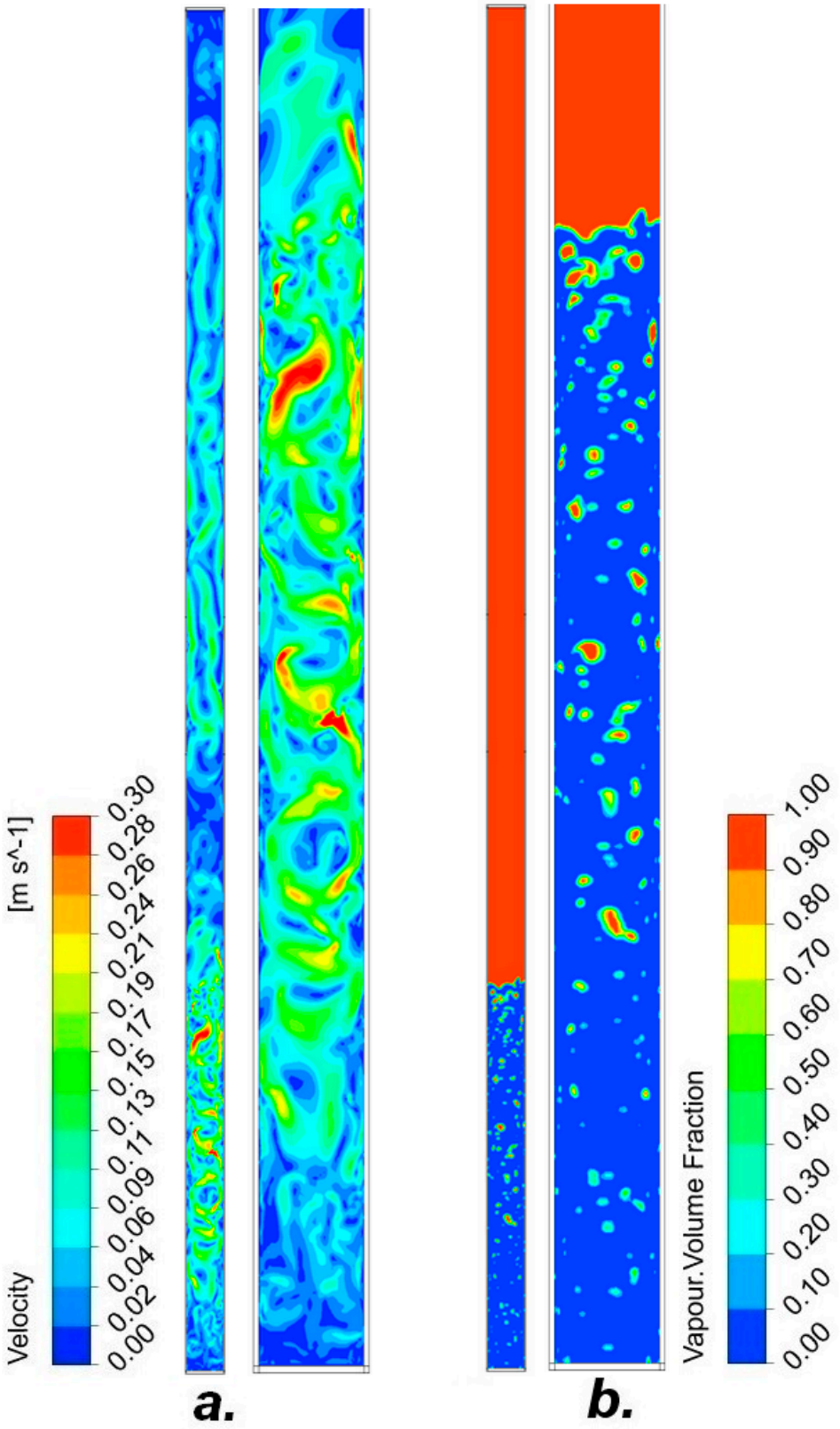

Figure 33. (**a**) Fluid velocity in the total heat pipe and in the condenser section, (**b**) the volume fraction of steam in the total heat pipe and in the evaporator section.

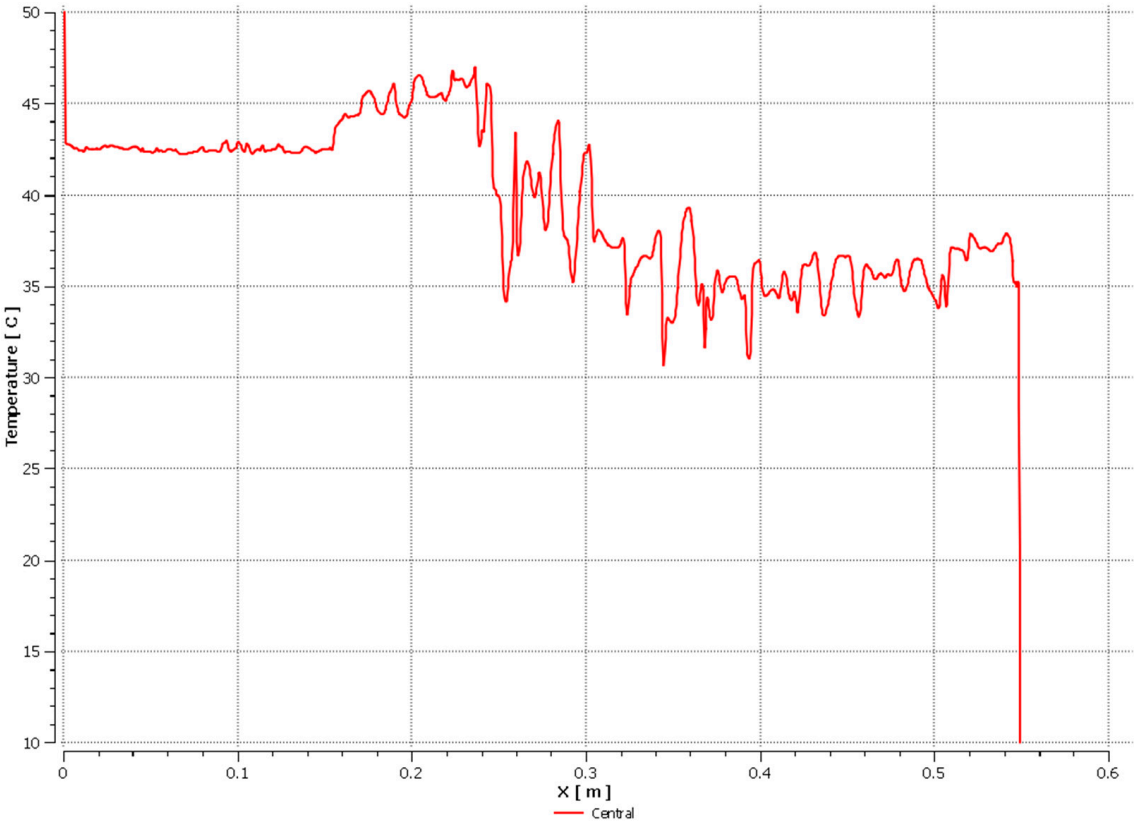

Figure 34. Temperature distribution along the height of the heat pipe's central line.

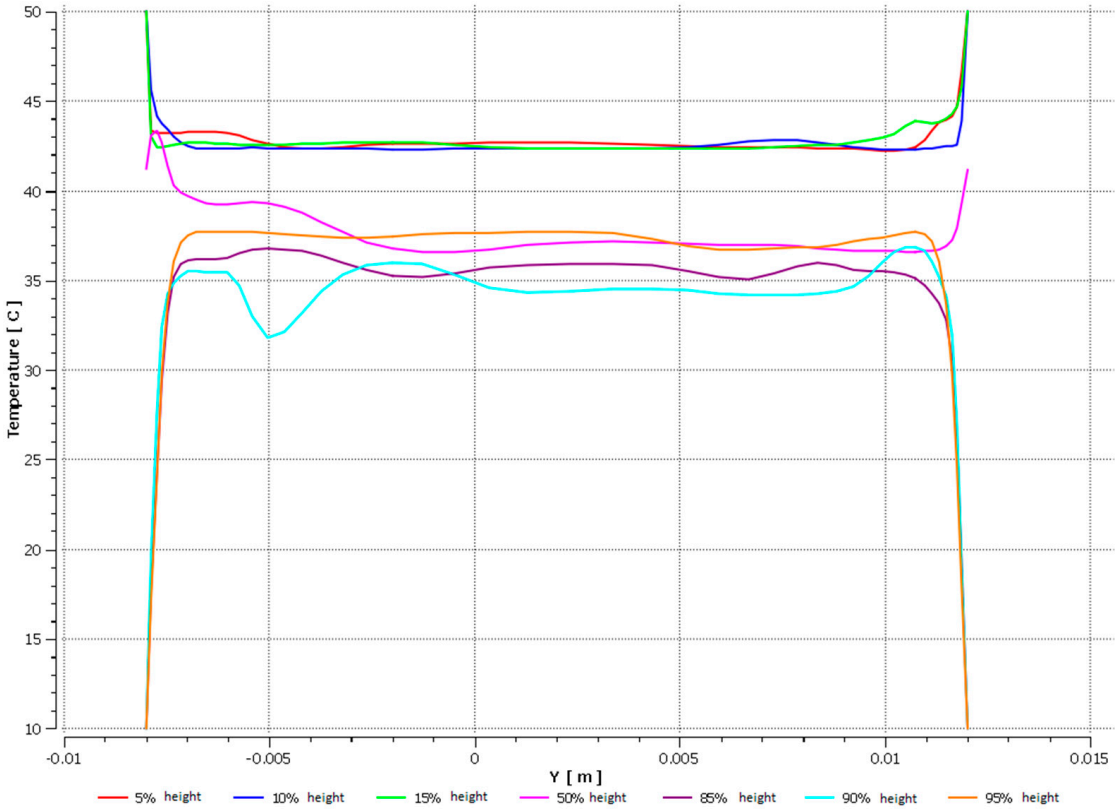

Figure 35. Temperature distribution along the cross-section.

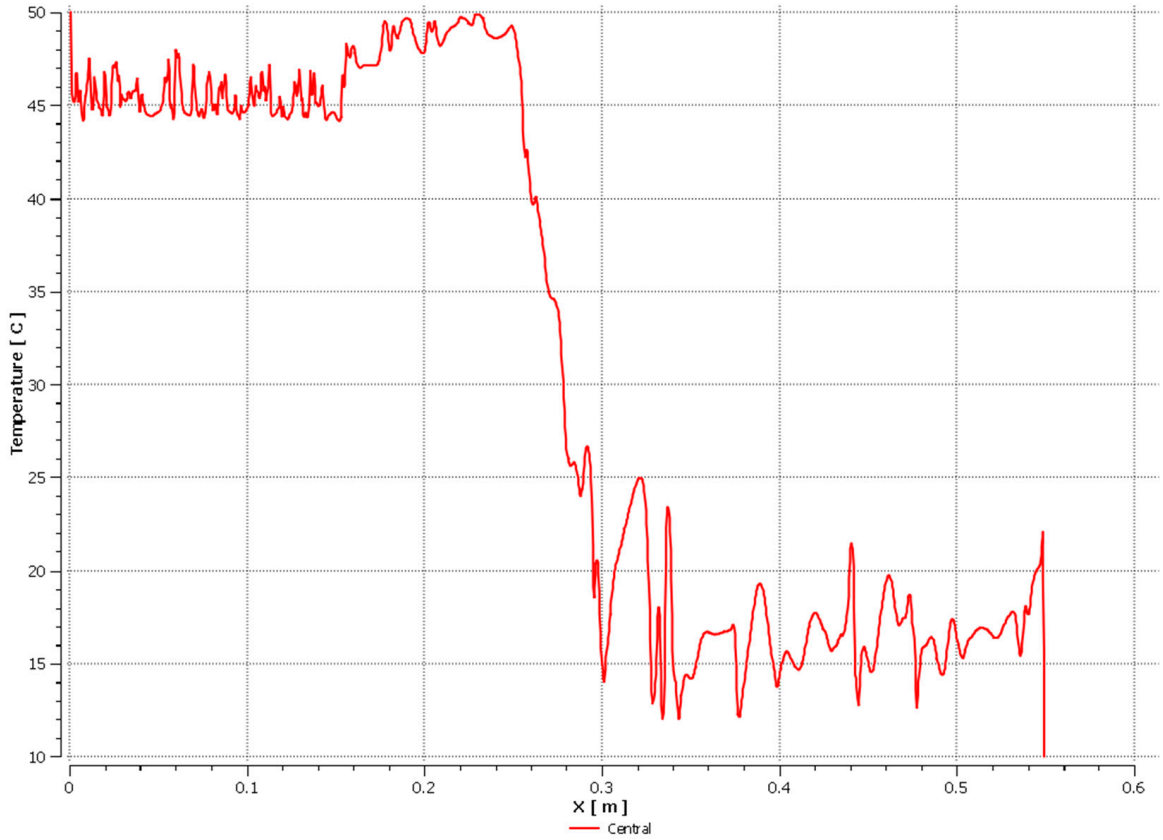

Figure 36. Temperature distribution along the height of the heat pipe's wall.

4. Discussion

Numerical methods of studying Heat Pipes are not the subject of many scientists' work, mainly due to the complexity of the processes taking place inside them at the same time. In their research, Chen and other co-authors [7] built a theoretical model of a heat pipe, the results of which are similar to the results presented in this publication. On the other hand, Qian [8] presented a three-dimensional numerical model based on similar numerical assumptions presented in this publication. In Ref. [9], Gao and co-authors focused on the structural design of the catalytic zone of the sulfuric acid decomposition plant. The double inner tube was designed to analyze the effects of the heat transfer surface of the inner tube and the catalytic volume of the ring area on the decomposition rate. The results show that the new design meets the decomposition temperature requirements and increases the heat flow rate, and validates the use of heat pipes. On the other hand, Kim and co-authors in [10] studied heat exchangers with parallel flow with collectors, which are widely used in various industries due to their compact size and ease of application. They conducted research to understand flow characteristics and improve flow distribution and pressure drop similar to this publication. In turn, Zhang and co-authors in [11] proposed an innovative design with dense ribs of less thickness in the upper layer and relatively low ribs of greater thickness in the lower layer to further improve the overall thermal efficiency of a two-layer microchannel heat exchanger; the numerical model was based on similar equations presented in this publication. In the works on numerical modeling [12–15], the authors use numerical models to optimize heat exchangers, both traditional and heat pipes, and obtain results similar to the results obtained in this publication. Rossome and Ochman, together with their co-authors in [16,17], study numerical processes of heat exchange in thermal energy stores. On the other hand, the authors of [18–22] numerically investigate the processes taking place in heat pipes for specific applications and for individual processes taking place inside heat pipes, where similar processes can be observed to those observed

in this publication. In turn, the authors of the works [23–25] investigate the basic processes of heat exchange also taking place in heat pipes and look at these processes on the example of heat storage. In turn, Fydrych [26] discussed heat exchange processes in cryogenic conditions for which heat pipes can be an ideal application.

4.1. Discussion on the Operation of the Heat Pipe with the Use of Low-Boiling Agents

4.1.1. Heat Pipe with Air

Due to the negligible heat transfer, the tube is completely ineffective, and the mere heat conduction through the wall of the tube along its length is negligible.

4.1.2. Heat Pipe with Low-Boiling Factors

As a result of computer simulations, the turbulent nature of the flow can be observed. This is evidenced by both the swirls visible in the temperature profile and the jagged graph of temperature distributions. From a heat transfer point of view, this is great news—higher turbulence means higher heat transfer coefficients. Additionally, there are no special observations in the tube axis, which means that there is no flow channeling [27]. Moreover, there is an asymmetry in the diagrams, which indicates a slightly different course of the process in the lower and upper parts of the exchanger. Some are related to additional effects, e.g., phase changes, while some result from other process parameters due to a different temperature [28]. The simulation results show a fairly linear temperature in the cross-sections of the tube at different heights. In principle, this indicates turbulent flow and no significant thermal resistance gradient along the radius of the tube. On the other hand, a sharp change in temperature in the isothermal section confirms the correct mechanism of operation of the heat pipe heat exchanger. There is also little confusion at the walls due to the lack of roughness and the flow of the liquid down the wall of the heat tube [29].

5. Conclusions

The presented numerical model of the heat pipe and the results of computer simulations are a continuation, as well as an attempt to visualize the experimental tests for the tested heat pipe geometries, as well as the presented work factors and their best filling levels, selected on the basis of experimental tests [6]. Computer simulations also confirmed the negligible heat transfer through a heat pipe filled with air, which is also the same as the results of experimental studies [30]. Based on the analysis of the presented results for the tested geometries and working media, it can be stated with certainty that the presented numerical model of the heat pipe, as well as computer simulations, can be used to analyze other geometries of heat pipes and various working factors and their degrees of filling with a high probability of obtaining similar results to reality.

As part of this study, on the basis of a numerical model and computer simulations, the issues related to the analysis of the efficiency of heat pipes in order to optimize heat transfer processes were analyzed. Based on the simulation results, it has been proven that the analysis of the processes taking place in heat pipe heat exchangers will allow the selection of the most optimal working medium and amounts, which will allow for maximum efficiency in a given temperature range.

The presented numerical model and computer simulations made it possible to draw a number of conclusions regarding heat pipes. These conclusions mainly concern:

- Selection of the most optimal working medium and its amount in a given temperature range.

Based on the analysis of computer simulations, it should be concluded that the most optimal working medium of the heat pipe No. I in the tested temperature range is the working medium R134A with 10% filling of the heat pipe. The efficiency of the heat pipe for this factor and its filling was from 90% to 95%. The obtained simulation results indicate the point character of the factor evaporation process, where the phase change occurs mainly in the foci. Furthermore, it is noteworthy that the very intense steam movement near the walls was in the condenser part of the heat pipe. Along with the observable changes in the temperature of these walls, it can be concluded that an intense heat exchange takes place

on their surface, and thus a change in the phase of the working medium is visible. Among the working media tested for brass heat pipes 550 mm in length and 22 mm in diameter, R404A is the most optimal refrigerant for use with 10% filling. The working medium in the form of the R407C refrigerant turned out to be the least effective factor among the respondents, which, when implemented in the heat pipe, was characterized by low heat exchange efficiency in the given temperature range.

- Efficiency of the heat pipes and the value of the heat flux transmitted by them. Based on the numerical model and computer simulations, it can be concluded that the 1769 mm long heat pipe is preferable to the 550 mm long heat pipe by comparing the most advantageous types and amounts of working media used in them. The heat pipe made of copper was more efficient and generated greater temperature differences, which is mainly due to a larger heat exchange surface on both the evaporator and condenser sides.
- Usefulness of using heat exchangers of the heat tube type. Heat pipes can be used in many industries, mainly where effective heat transport is needed without direct contact of factors with each other. An example of this is, for example, phase change materials, which offer a very large heat storage capacity and are capable of quickly absorbing and releasing heat. The problem with the use of phase change materials is the heat exchange between them and the factor supplying and receiving heat from them. The contact of the factor with the materials is often unacceptable, and they do not currently use the full ability to receive and give off heat by phase change materials, for example, in heat and cold stores. Therefore, a series of numerical analyses and computer simulations were necessary to analyze the operation of heat pipes and determine the most optimal heat exchangers of the heat pipe type depending on their operating conditions. The results of computer simulations will enable the selection of heat pipes for a given temperature range of their operation and will allow estimation of their efficiency and the power of the transferred heat flux.

Author Contributions: Conceptualization, Ł.A., S.S., P.P. and F.M.; methodology, Ł.A., S.S. and P.P.; software, Ł.A. and F.M.; validation, Ł.A., S.S., P.P. and F.M.; formal analysis, Ł.A., S.S. and P.P.; investigation, Ł.A., S.S. and F.M.; resources Ł.A., S.S. and P.P.; data curation, Ł.A., S.S. and P.P.; writing—original draft preparation, Ł.A., S.S., P.P. and F.M.; writing—review and editing, Ł.A., S.S., P.P. and F.M.; visualization, Ł.A., S.S. and P.P.; supervision, Ł.A., S.S. and P.P.; project administration, Ł.A., S.S. and P.P.; funding acquisition, Ł.A., S.S. and P.P. All authors have read and agreed to the published version of the manuscript.

Funding: This research received no external funding.

Institutional Review Board Statement: Not applicable.

Informed Consent Statement: Not applicable.

Data Availability Statement: Not applicable.

Acknowledgments: NCN GRANT: Preludium II no: DEC-2011/03/N/ST8/05912 pt. "Research on heat exchange processes and distribution of velocity fields by the PIV method and the effects of phase changes and capillary transport occurring in heat exchangers of the heat tube type". The grant was financed by the National Science Center in Krakow.

Conflicts of Interest: The authors declare no conflict of interest.

Nomenclature

S_m	Volume sources
g	Gravitational acceleration
F	External forces acting on the fluid
p	Pressure, Pa
m_{pq}, m_{qp}	Mass flows between phases
T_l	Liquid temperature, °C
T_g	Gas temperature, °C
T_{sat}	Saturation temperature, °C
$\dot{m}_{lv}$	Volumetric mass source
$Coef$	Empirical coefficient
k	Thermal conductivity, W/(m·K)
h	Heat transfer coefficient, W/(m^2·K)
R	Thermal resistance, K/W
f	Friction coefficient
ν	Kinematic viscosity, m^2/s
ρ	Density, kg/m^3
Nu	Nusselt number
Pr	Prandlt number
Q	Heat transfer rate through heat pipe, W
Q_H	External source of heat, W
C_μ	Model coefficient, dependent on flow type
u	Fluid velocity, m/s
S_{ij}	Reynolds-averaged strain-rate tensor
q	Heat flux density
y	Distance from point to the wall, m
tz1	Cold water temperature at the inlet to the cooling exchanger, °C
tz2	Cold water temperature at the outlet from the cooling exchanger, °C
tg1	Hot water temperature at the entrance to the heat exchanger, °C
tg2	Hot water temperature at the outlet of the heating exchanger, °C
trz	Heat pipe wall temperature in the center of the condensing section, °C
trg	Heat pipe wall temperature in the center of the evaporating section °C
Greek Symbols	
τ	Viscous stress
α_q	Volume fraction of q-phase in the cell
Indices	
v	Vapour
l	Liquid
ij	Matrix coordinates

References

1. Eurostat. *Sustainable Development in the European Union—Monitoring Report on Progress towards the SDGs in an EU Context—2021 Edition*; Publications Office of the EU: Luxembourg, 2021. [CrossRef]
2. Eurostat. *Environmental Goods and Services Sector Accounts—Handbook 2016 Edition*; Publications Office of the EU: Luxembourg, 2016. [CrossRef]
3. Eurostat. *Panorama of Energy; Environment and Energy; Collection: Statistical Books*; Eurostat: Luxembourg, 2009; ISBN 978-92-79-11151-8.
4. Eurostat. *Handbook on Environmental Goods and Services Sector*; Eurostat: Luxembourg, 2009; ISSN 1977-0375.
5. Wu, X.P.; Johnson, P.; Akbarzadeh, A. Application of heat pipe heat exchangers to humidity control in air-conditioning systems. *Appl. Therm. Eng.* **1997**, *17*, 561–568. [CrossRef]
6. Adrian, Ł.; Szufa, S.; Piersa, P.; Kuryło, P.; Mikołajczyk, F.; Kurowski, K.; Pochwała, S.; Obraniak, A.; Stelmach, J.; Wielgosiński, G.; et al. Analysis and Evaluation of Heat Pipe Efficiency to Reduce Low Emission with the Use of Working Agents R134A, R404A and R407C, R410A. *Energies* **2021**, *14*, 1926. [CrossRef]
7. Chen, Q.; Shi, Y.; Zhuang, Z.; Weng, L.; Xu, C.; Zhou, J. Numerical Analysis of Liquid–Liquid Heat Pipe Heat Exchanger Based on a Novel Model. *Energies* **2021**, *14*, 589. [CrossRef]
8. Qian, Z.; Wang, Q.; Lv, S. Research on the Thermal Hydraulic Performance and Entropy Generation Characteristics of Finned Tube Heat Exchanger with Streamline Tube. *Energies* **2020**, *13*, 5408. [CrossRef]

9. Gao, Q.; Zhang, P.; Peng, W.; Chen, S.; Zhao, G. Structural Design Simulation of Bayonet Heat Exchanger for Sulfuric Acid Decomposition. *Energies* **2021**, *14*, 422. [CrossRef]
10. Kim, B.; Kim, K.; Kim, S. Numerical Study on Novel Design for Compact Parallel-Flow Heat Exchanger with Manifolds to Improve Flow Characteristics. *Energies* **2020**, *13*, 6330. [CrossRef]
11. Zhang, Y.-D.; Chen, M.-R.; Wu, J.-H.; Hung, K.-S.; Wang, C.-C. Performance Improvement of a Double-Layer Microchannel Heat Sink via Novel Fin Geometry—A Numerical Study. *Energies* **2021**, *14*, 3585. [CrossRef]
12. Teodori, E.; Pontes, P.; Moita, A.; Georgoulas, A.; Marengo, M.; Moreira, A. Sensible Heat Transfer during Droplet Cooling: Experimental and Numerical Analysis. *Energies* **2017**, *10*, 790. [CrossRef]
13. Song, E.-H.; Lee, K.-B.; Rhi, S.-H. Thermal and Flow Simulation of Concentric Annular Heat Pipe with Symmetric or Asymmetric Condenser. *Energies* **2021**, *14*, 3333. [CrossRef]
14. Pang, L.; Luo, K.; Yu, S.; Ma, D.; Zhao, M.; Mao, X. Study on Heat Transfer Performance of Antifreeze-R134a Heat Exchanger (ARHEx). *Energies* **2020**, *13*, 6129. [CrossRef]
15. Yang, J.; Zhao, Y.; Chen, A.; Quan, Z. Thermal Performance of a Low-Temperature Heat Exchanger Using a Micro Heat Pipe Array. *Energies* **2019**, *12*, 675. [CrossRef]
16. Ochman, A.; Chen, W.-Q.; Błasiak, P.; Pomorski, M.; Pietrowicz, S. The Use of Capsuled Paraffin Wax in Low-Temperature Thermal Energy Storage Applications: An Experimental and Numerical Investigation. *Energies* **2021**, *14*, 538. [CrossRef]
17. Rossomme, S. Modélisation de L'éVaporation Des Lms Liquides Minces, Y Compris AU Voisinage Des Lignes de Contact: Application Aux Caloducs à Rainures. Ph.D. Thesis, Université libre de Bruxelles, Bruxelles, Belgique, 2008.
18. Kaya, M. An experimental investigation on thermal efficiency of two-phase closed thermosyphon (TPCT) filled with CuO/water nanofluid. *Eng. Sci. Technol. Int. J.* **2020**, *23*, 812–820. [CrossRef]
19. Wong, S.-C. *The Evaporation Mechanism in the Wick of Copper Heat Pipes*; Springer: Berlin/Heidelberg, Germany, 2014; ISBN 978-3-319-04494-1. [CrossRef]
20. Haque, M.E.; Efthakher, M.; Mashud, H. Performance Analysis of a Heat Pipe with Stainless Steel Wick. *J. Eng. Adv.* **2020**, *1*, 16–22. [CrossRef]
21. Schepper, S.C.K.; Heynderickx, G.J.; Marin, G.B. CFD modeling of all gas–liquid and vapor–liquid flow regimes predicted by the Baker chart. *Chem. Eng. J.* **2008**, *138*, 349–357. [CrossRef]
22. Smirnov, H.; Henry, F. *Transport Phenomena in Capillary-Porous Structures and Heat Pipes*; CRC Press: Boca Raton, FL, USA, 2010. [CrossRef]
23. Nowak-Ocłoń, M.; Ocłoń, P. Thermal and economic analysis of preinsulated and twin-pipe heat network operation. *Energy* **2020**, *193*, 116619. [CrossRef]
24. Ochman, A.; Pietrowicz, S. The thermal behaviour of a special heat exchanger filled with the phase change material dedicated for low—Temperature storage applications. In *EPJ Web of Conferences*; EDP Sciences: Les Ulis, France, 2019. [CrossRef]
25. Smakulski, P.; Pietrowicz, S.; Ishimoto, J. The numerical modeling of cell freezing in binary solution under subcooling conditions. *Int. J. Numer. Methods Heat Fluid Flow* **2020**, *30*, 3005–3025. [CrossRef]
26. Fydrych, J.; Pietrowicz, S. A comparative thermodynamic analysis of helium distribution systems with central and distributed precooling heat exchangers. *IOP Conf. Ser. Mater. Sci. Eng.* **2019**, *502*, 012173. [CrossRef]
27. Adrian, Ł.; Piersa, P.; Szufa, S.; Romanowska-Duda, Z.; Grzesik, M.; Cebula, A.; Kowalczyk, S.; Ratajczyk-Szufa, J. Experimental research and thermographic analysis of heat transfer processes in a heat pipe heat exchanger utilizing as a working fluid R134A. In *Renewable Energy Sources: Engineering, Technology, Innovation*; Mudryk, K., Werle, S., Eds.; Springer Proceedings in Energy ICORES 2017; Springer: Cham, Switzerland, 2018; pp. 413–421. ISBN 978-3-319-72370-9. [CrossRef]
28. Głogowski, M.; Kubiak, P.; Szufa, S.; Piersa, P.; Adrian, Ł.; Krukowski, M. The Use of the Fourier Series to Analyze the Shaping of Thermodynamic Processes in Heat Engines. *Energies* **2021**, *14*, 2316. [CrossRef]
29. Siuda, R.; Kwiatek, J.; Szufa, S.; Obraniak, A.; Piersa, P.; Adrian, Ł.; Modrzewski, R.; Ławińska, K.; Siczek, K.; Olejnik, T.P. Industrial verification and research development of lime-gypsum fertilizer granulation method. *Minerals* **2021**, *11*, 119. [CrossRef]
30. Adrian, Ł.; Szufa, S.; Piersa, P.; Romanowska-Duda, Z.; Grzesik, M.; Cebula, A.; Kowalczyk, S.; Ratajczyk-Szufa, J. Thermographic analysis and experimental work using laboratory installation of heat transfer processes in a heat pipe heat exchanger utilizing as a working fluid R404A and R407A. In *Renewable Energy Sources: Engineering, Technology, Innovation*; Wróbel, M., Jewiarz, M., Szlęk, A., Eds.; Springer Proceedings in Energy; Springer: Cham, Switzerland, 2020; pp. 799–807. ISBN 978-3-030-13887-5. [CrossRef]